Insights into Chemically Fueled Supramolecular Polymers

Anastasiia Sharko, Dimitri Livitz, Serena de Piccoli, Kyle J. M. Bishop, Thomas Hermans

Insights into chemically-fueled supramolecular polymers

Anastasiia Sharko,[†,#] Dimitri Livitz,[‡,#] Serena De Piccoli,[†,#] Kyle J. M. Bishop,[*,‡] and Thomas M. Hermans[*,†]

[†]University of Strasbourg & CNRS, UMR7140, Strasbourg, France

[‡]Department of Chemical Engineering, Columbia University, New York, USA

[*] kyle.bishop@columbia.edu, hermans@unistra.fr

[#]equal contributions

Abstract

Supramolecular polymerization can be controlled in space and time by chemical fuels. A non-assembled monomer is activated by the fuel and subsequently self-assembles into a polymer. Deactivation of the molecule either in solution or inside the polymer leads to disassembly. Whereas biology has already mastered this approach, fully artificial examples have only appeared in the past decade. Here, we map the available literature examples into four distinct regimes depending on their activation/deactivation rates and the equivalents of deactivating fuel. We present increasingly complex mathematical models, first considering only the chemical activation/deactivation rates (i.e., Transient Activation), and later including the full details of the isodesmic or cooperative supramolecular processes (i.e., Transient Self-assembly). We finish by showing that sustained oscillations are possible in chemically fueled cooperative supramolecular polymerization and provide mechanistic insights. We hope our models encourage the quantification of activation, deactivation, assembly, and disassembly kinetics in future studies.

1. Introduction

1.1 Inspiration from Nature

Living organisms use food to build cellular components, eliminate metabolic waste, and generate energy carriers like adenosine triphosphate (ATP) and guanosine triphosphate (GTP). The latter are used by a vast range of energy-transducing enzymes, molecular motors, pumps, and filaments to enable complex cell functions, such as signaling, self-healing, motility, and division. Particularly interesting to the topic of this article are cytoskeletal structures such as actin filaments and microtubules, which are supramolecular polymers that undergo dissipative self-assembly. For example, GTP-bound tubulin dimers undergo an entropically driven polymerization process to form microtubules of 25 nm diameter and micrometer length.[1] The tubulin dimer, however, is also an enzyme that hydrolyses GTP to guanosine diphosphate (GDP) and inorganic phosphate, with increased activity when surrounded by other GTP-dimers. The dimer changes from a straight to a tilted conformation during the latter hydrolysis reaction, resulting in a spring-loaded microtubule structure.[2] GTP-dimers located at the growing (+)-end of the microtubule (a "GTP cap"), however, force the structure to remain straight due to a high kinetic barrier. Eventually, when the (local) solution concentration of GTP-dimers decreases, the GTP cap is removed and the microtubule undergoes a catastrophic breakdown. Microtubules nucleate from a microtubule-organizing center (MTOC)—often located at the centroid of the cell—forming flower-like structures reminiscent of asters. Interestingly, in cell-free reconstituted systems, this centering function can be reproduced in microscopic glass chambers using just tubulin dimers and GTP.[3,4] The tubes emanating from the MTOC push against the chamber walls and reach a steady-state where the sum of all forces is zero (i.e., the centroid). The centering can be further improved by adding pulling forces, mediated by dynein motor proteins at the chamber walls.[5]

Microtubules have captured the imagination of many supramolecular chemists since their structure is phenomenally stiff (persistence length of > 1 mm) and yet they polymerize and depolymerize on the minute timescale. They allow the cell to withstand compressive loads, but also become more fluid when the time comes for it to move. They can nucleate at specific locations to sense and exert mechanical forces and can self-repair from their ends or sides while doing so. A little over a decade after the first artificial microtubule-like system,[6] the field of (supramolecular) Systems Chemistry has rapidly developed into an area where chemical fuels and light are used to assemble and disassemble supramolecular polymers, vesicles, colloids, and nanoparticles. Unlike biology, synthetic chemists are not restricted to natural fuels like ATP and GTP, amino acid building blocks, or even to aqueous solvents. The past decade has seen an exploration of suitable chemistries, switches, and monomers that can reproduce some aspects of dissipative self-assembly that make microtubules so mesmerizing (see recent reviews [7–11]).

For the most part, the systems developed so far undergo transient self-assembly, where an aliquot of fuel or a light pulse leads to (chemical) 'activation' of a monomer, which assembles for a given time and spontaneously 'deactivates' and disassembles without further experimental intervention (e.g., changing temperature, pH, illumination, etc.). For example, an activation reaction can remove the ionic charge of a monomer and thus induce self-assembly, by suppression of Coulombic repulsion. A second deactivating reaction then restores the charge and triggers disassembly. This and related approaches have led to interesting new properties such as self-erasing inks[12–14], timed drug release[15–18], temporary 'artery clamping'[19,20], and transient catalysis[21,22]. Still, we are currently in the Rube Goldberg era of artificial dissipative self-assembly: performing simple tasks, like assembly and disassembly, in overly complicated and inefficient ways. Fortunately, it is likely that our methods will continue to improve, and that at some point we will be able to construct systems and materials with complexity and functionality approaching that of biological matter.

1.2 Aim

One aspect that is sure to enhance our progress is the proper quantitative understanding of how chemical reactions (or light) can be 'coupled' to the self-assembly of supramolecular structures. In recent years, 'toy models'[23–26] that consider the steady-state dimerization of species have been put forward to classify dissipative self-assembly based on how chemical energy is stored in thermodynamically unfavorable states (inspired by energy/information ratchets in biological systems[27,28]; see also work on molecular motors[23]). In addition, several numerical studies have been devoted to this topic[29,30] as well as perspectives[10,31–36].

The aim of our current work is to show how coupling of fueled reactions and self-assembly can be understood quantitatively using mathematical models. We will show that the characteristic 'hump' of transient self-assembly, fuel depletion, and disassembly (i.e., monomer→assembly→monomer in time) can be achieved in different ways. Based on the sparse kinetic data available, we map current literature examples of Transient Self-assembly according to their activation/deactivation rates and the equivalents of fuel molecules. The main text presents only the simple analytical solutions of the models where possible. The full mathematical derivations can be found in the Supporting Information, which can be read as a standalone paper (recommended for physical chemists or supramolecular polymer physicists). We will limit our analysis to one-dimensional supramolecular polymers in homogeneous environments but include literature examples that are somewhat broader. In particular, we would like to point the reader to many other efforts addressing higher dimensional systems such as vesicles, nanoparticles, nanoparticle superlattices, DNA origami, etc.[37–78]. Before going into detail in sections 2–4, we first explain what we mean by 'coupling' and introduce the important processes needed later on.

1.3 Coupling to self-assembly

We distinguish four important factors that are frequently encountered in Dissipative Self-assembly (see Fig. 1a): i) mechanisms to activate and deactivate a monomer, i.e., [Reaction], ii) assembly and disassembly of the monomer into supramolecular structures, i.e., [Assembly], iii) solution conditions like pH or ionic strength, i.e., [Medium], and iv) mass transport phenomena such as gas-to-liquid transfer or slow addition of chemical species, i.e., [Transport] in Figure 1a.

It is well-known in the field of Supramolecular Chemistry that the medium has a large influence on the state of self-assembly, which we denote as [Medium]→[Assembly]. The reverse [Assembly]→[Medium] is usually not considered; any relevant molecule in the medium would be included to evaluate the Gibbs free energy (ΔG), and would therefore be part of [Assembly]. The [Medium]→[Assembly] influence is the basis of most stimuli-responsive materials.[79] For example, poly(*N*-iso-propylacrylamide)-based systems make use of the temperature-dependent phase behavior of the polymer. Below the lower critical solution temperature, the polymer is soluble and expanded, whereas above this temperature, it becomes insoluble and collapses resulting in aggregation. Chemical reactions can be used to change the solution environment and thereby influence the state of self-assembly. For example, spontaneous ring-opening *activation* of glucono-δ-lactone lowers the pH of the *medium* and causes *assembly* of monomers into well-organized hydrogels ([Reaction]→[Medium]→[Assembly] in Fig. 1).[80] The novelty in the field of Dissipative Self-assembly is to engineer systems that complete a full cycle from a disassembled state to an assembled state and back without experimental intervention. This autonomous cycling is the clear distinguishing factor when compared to existing stimuli-responsive materials, where the original stimulus needs to be reversed or compensated by the experimentalist(s).

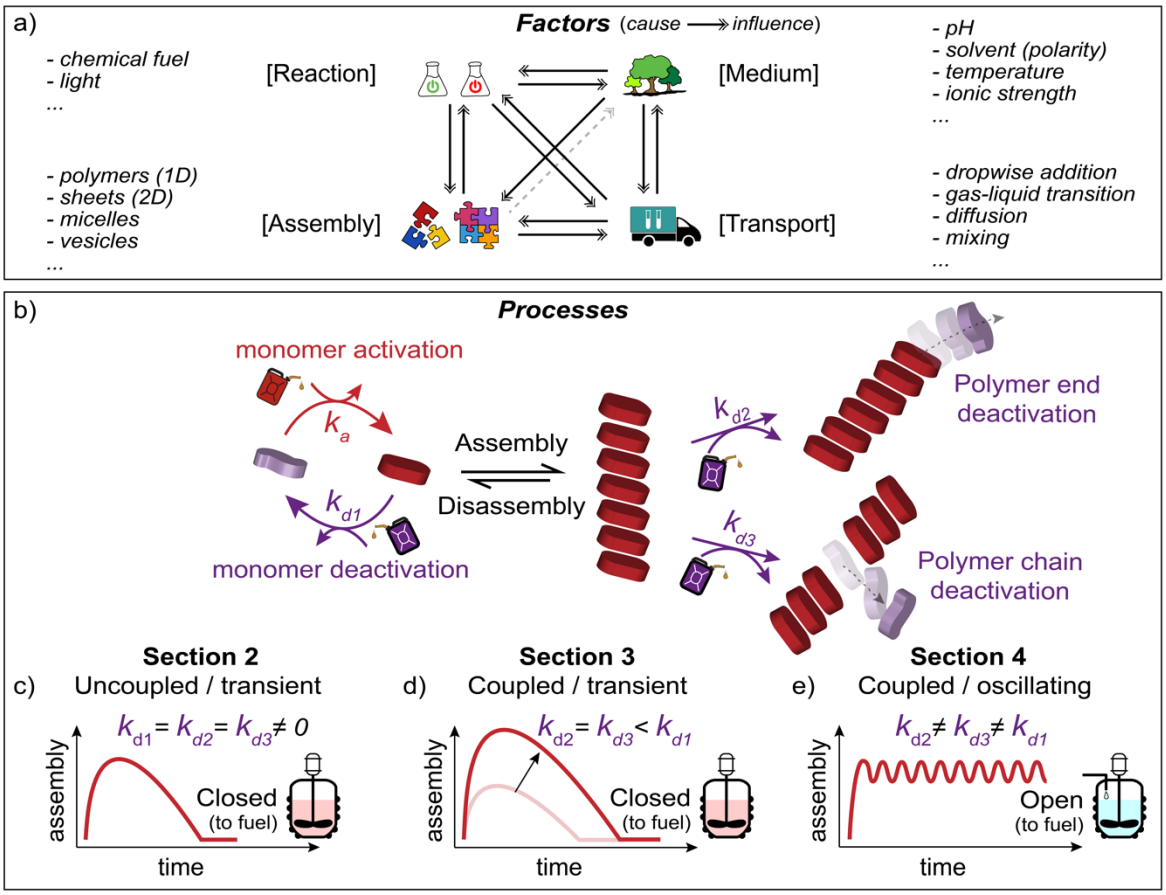

Figure 1 | Factors and processes in dissipative self-assembly. a) Factors of importance: chemical activation or deactivation reactions [Reaction], self-assembly or disassembly [Assembly], solution conditions [Medium], and mass transport phenomena [Transport]. Arrows indicate causal influence. See the main text for more details. The dashed arrow from [Assembly]→[Medium] is an unlikely causation; b) The key processes that will be used in the various models in this paper. The key rate constants are k_a (activation), k_{d1} (monomer deactivation), k_{d2} (polymer end deactivation), k_{d3} (polymer chain deactivation). c) Transient activation uncoupled from self-assembly: see section 2, d) Transient self-assembly with coupling: see section 3, e) Oscillations in coupled dissipative self-assembly: see section 4 of this work.

By considering the causal influences between these different factors and neglecting all but the most important, one can greatly simplify the analysis and understanding of Dissipative Self-Assembly. For example, when the causal influence [Assembly]→[Reaction] is neglected, the rates of chemical activation and/or deactivation reactions are assumed to be independent of the assembly

state. As a result, one can hope to understand the transient processes of activation and deactivation without reference to those of assembly and disassembly. We refer to such idealized systems as 'uncoupled'. In contrast, the coupling [Assembly]→[Reaction] occurs when the state of self-assembly affects the rate of deactivation—for example, by shielding monomers inside bundled fibers of which more later (see section 3.3 and 4). Coupling is also achieved when self-assemblies accelerate the rate of monomer activation/deactivation through their catalytic activity.[81]

1.4 Basic processes and outline

Some terminology such as 'chemical fuel' is used in a specific way in the field of Systems Chemistry, which is different from the definitions found in common dictionaries referring to a liquid releasing energy upon combustion. In the context of this paper, we use the definitions in Box 1 below.

Box 1 | Key definitions in chemically fueled self-assembly

Chemical fuel	A reactant that changes the molecular structure of a monomer by a chemical reaction –or– binds to the monomer non-covalently. An 'activating fuel' activates the monomer so it can assemble into supramolecular polymers. A 'deactivating fuel' removes the propensity of the monomer to assemble, eventually leading to disassembly of the polymer. Here, when we refer just to 'fuel', we mean the 'activating chemical fuel'.
Chemical waste	The chemical substances that remain (in solution, gas phase, or solid phase) after the activating fuel reacts with the deactivated monomer –or– the deactivating fuel reacts with the activated monomer. 'Waste' from activating or deactivating fuels in usually not distinguished. Often the build-up of chemical waste can dampen the system response in repeated cycles of transient self-assembly.[82]
Activation	The reaction of the activating fuel with the deactivated monomer, resulting in (chemical waste and) the activated monomer that can self-assemble into supramolecular polymers.

Deactivation	The deactivation of an activated monomer (either free in solution, at the ends of supramolecular polymers, or along the polymer chains) by the deactivating fuel, removing the propensity of the monomer to assemble (and producing waste).
Coupling	Interactions between chemical reaction(s) and self-assembly whereby one affects the other (or vice versa or both). See the main text for more details, and definitions used in molecular chemical engines[83] or biological molecular machines[84,85].

Looking at the relevant processes in more detail, a monomer can be activated with rate constant k_a, after which it can self-assemble into a supramolecular polymer (Figure 1b in red). We will consider both isodesmic as well as cooperative polymerization mechanisms. The monomer can be deactivated either in solution, at the polymer end, or somewhere along the chain of the polymer with rate constants k_{d1}, k_{d2}, and k_{d3}, respectively.

If the three deactivation rate constants are equal (and non-zero), the system is classified as 'uncoupled', and its 'Transient Activation' (section 2.1) proceeds independently from the simultaneous process of Transient Self-assembly (Figure 1c). Depending on the relative rates of activation, deactivation, and fuel consumption, we show that Transient Activation can proceed by four distinct mechanisms. Alternatively, if deactivation on the polymer is slower than in solution—as in the shielding example in the previous section—the 'coupled' system exhibits Transient Self-assembly over a wider range of experimental conditions (section 2.2). We have mapped the currently available literature examples that fall within the constraints of our models onto a phase space describing the relative rates of activation/deactivation and the number of fuel equivalents (Figure 2), which leads to interesting insights (section 3).

The most complex behavior emerges when chemically fueled [Assembly]→[Reaction] coupling is combined with cooperative polymerization—i.e., including nucleation, elongation, fragmentation etc.—to produce sustained oscillations in the number and length of polymer

assemblies (section 4). We conclude with a summary of insights and lessons learned from the analysis of simple models and discuss the possible impacts of our findings on future supramolecular materials (section 5).

2. Transient Activation uncoupled from Self-assembly

2.1 Model

In general, experimental systems showing transient self-assembly often consist of i) an activation phase, where (usually low molecular weight) building blocks are turned "on" and assemble into well-defined structures, ii) possibly a short plateau where conditions stay approximately constant, and iii) a deactivation and disassembly phase. Depending on the concentration of the assembling species, these processes first lead to supramolecular polymers followed by a sol–gel–sol transition (due to non-covalent interactions between the polymers, see reference[86]). In other systems, a reverse process has been implemented, where self-assembled structures are initially present and are transiently deactivated and disassembled. That specific scenario can lead to a time-programmable gel–sol–gel behavior. In this section, we examine how the kinetics of (de)activation and (dis)assembly must be tuned to achieve the transient self-assembly 'hump' common to many reported systems. To do so, we consider a simple model of transient activation characterized by different parameter regimes that correspond to distinct dynamical behaviors. We map the kinetics of the reported systems onto these regimes and discuss their shared similarities in light of the model.

For simplicity, we start with an uncoupled model in which monomers are activated and deactivated irrespective of their position in solution or within polymer assemblies (see Supporting Information, Section 3). In this 'Transient Activation' model, deactivated monomer D is activated by reacting with activating chemical fuel F, leading to active monomer A that can form self-assembled structures. A is deactivated back to D by reaction with a second deactivating chemical

fuel G. These activation and deactivation reactions are approximated as irreversible with second order rate constants k_a and k_d, respectively,

$$\mathrm{D} + \mathrm{F} \xrightarrow{k_a} \mathrm{A} + \mathrm{P}$$

$$\mathrm{A} + \mathrm{G} \xrightarrow{k_d} \mathrm{D} + \mathrm{P}'$$

Here, P and P′ denote waste products, which are not relevant to the system's dynamics. We consider the time evolution of the species concentrations—denoted by italic lower case letters a, d, f, g—within a well-mixed batch reactor. Assuming a large excess of deactivating fuel G (e.g., for solvent mediated reactions like hydrolysis), the concentrations of activated monomer A and activating fuel F are governed by the following kinetic equations

$$\dot{a} = k_a f (c_{tot} - a) - k_d' a \tag{1}$$

$$\dot{f} = -k_a f (c_{tot} - a) \tag{2}$$

where $c_{tot} = a + d$ is the total monomer concentration, and $k_d' = k_d g$ is the pseudo-first order rate constant for deactivation. Initially, at time $t = 0$, all monomers are in their deactivated state $a(0) = 0$, and the fuel concentration is equal to a specified value $f(0) = f_0$.

According to this model, the degree of activation a / c_{tot} rises in time as monomers are converted to their activated form and then falls due to consumption of the activating fuel F. The details of this characteristic activation 'hump'—for example, how fast and high it rises and for how long it lasts—depend on the rate constants k_a and k_d' and the concentrations c_{tot} and f_0. In particular, the *qualitative* behavior of the system depends on just two dimensionless groups: i) $k_d'/k_a c_{\mathrm{tot}}$, the ratio between the rate of deactivation and the characteristic rate of activation, and ii) f_0/c_{tot}, the ratio between the initial fuel concentration and the total monomer concentration. Depending on the magnitudes of these groups, we identify four distinct regimes for transient activation (I-green, II-red, III-yellow, IV-blue in Fig. 2a). On this plot, the x-axis describes the relative speed of

deactivation relative to that of activation; the y-axis describes the amount of activating fuel relative to that of the building blocks. Below we describe each of these regimes in turn, highlighting representative examples from the literature. Details explaining how kinetic rate parameters were extracted from literature references are provided in the Supporting Information, Section 6. Briefly, we analyzed the kinetic profiles of transient systems obtained by any means of characterization (UV, CD, fluorescence, HPLC, NMR, rheology, pH profile, etc.), extracting apparent rate constants of (de)activation processes as well as the maximal degree of activation in each system. For systems where self-assembly strongly affects deactivation (see section 3), the mapping is not very accurate, but remains useful in a qualitative sense. In this section, we will first consider uncoupled systems (boxed numbers in Fig. 2a), for which the assembly does not have significant influence (positive or negative) on the rate of chemical activation and/or deactivation.

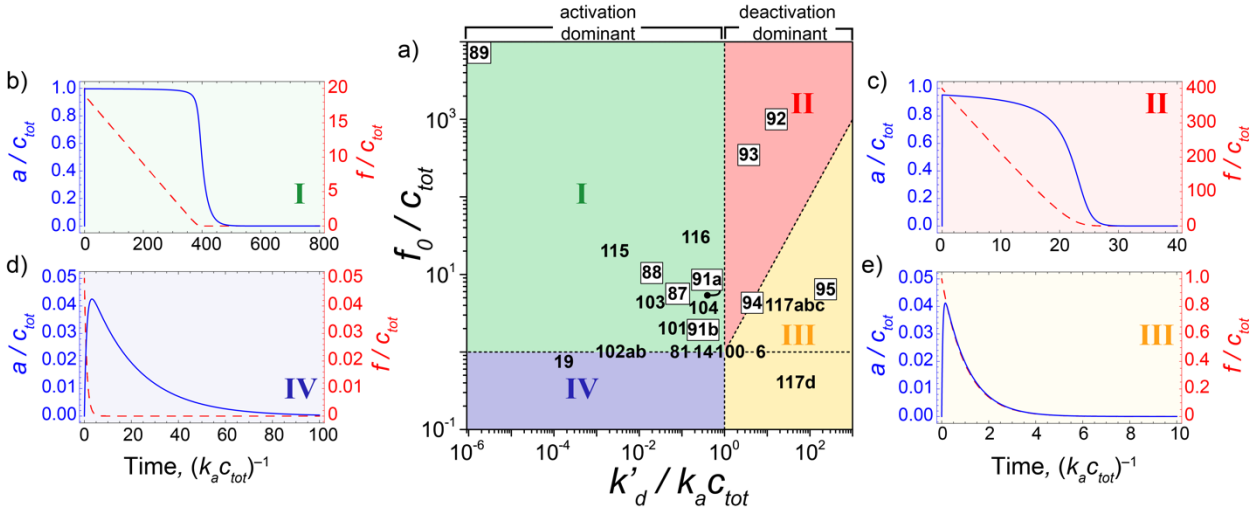

Figure 2: Regimes in chemically-fueled transient activation. a) Phase map showing four dynamical regimes for transient activation (solid green, red, yellow, and blue areas), which transition smoothly from one to another. The x-axis shows the relative rates of deactivation and activation, $k'_d/k_a c_{tot}$, where k'_d and k_a are the rate constants for deactivation and activation, respectively, and c_{tot} is the total monomer concentration. The y-axis shows the number of fuel equivalents, f_0/c_{tot}, where f_0 is the initial fuel concentration. Boxed numbers: uncoupled systems; unboxed numbers: coupled systems (see main text for description and definition). The numbers in the figure refer to the main text reference numbers. Typical time traces (solid lines show degree of activation a/c_{tot}, dashed lines are the dimensionless fuel concentration): b) Regime I: fast and full activation, c) Regime II: deactivation is fast, but since a

surplus of fuel is available, activation can still be high, d) Regime III: deactivation is dominant, and fuel is low to medium, e) Regime IV: fast deactivation, and not a lot of fuel leads to low activation and short transients. Time t is measured in units $(k_a c_{tot})^{-1}$; concentrations in units of c_{tot}.

2.2 Literature examples

Regime I.

We start in regime I where the conditions are perhaps the most intuitive for achieving transient activation. These systems are characterized by an excess of fuel with respect to the monomer ($f_0 \gg c_{tot}$) and by slow rates of deactivation relative to that of activation ($k_d' \ll k_a c_{tot}$). Starting from t = 0 (Fig. 2b), the monomer quickly reaches the fully activated state ($a \approx c_{\text{tot}}$). Despite continuous deactivation, high levels of activation are maintained for some time at the expense of continuous fuel consumption. Once the activating fuel is fully depleted, deactivation brings the system back to the initial (deactivated) state. In practice, a long plateau is not often observed, likely because experimentalists select for systems where the time scales for activation and deactivation are similar, as to achieve the characteristic 'hump'-like kinetics (monomer → assembly → monomer). Alternatively, the activating fuel may itself degrade or react with the deactivating fuel, thus prohibiting a long-lived plateau in the amount of activated monomer. Provided that self-assembly is fast relative to monomer deactivation, the transient activation kinetics predicted by this uncoupled model implies the transient assembly of activated building blocks and their subsequent disassembly upon deactivation.

An example by Adams and co-workers[87] shows a transient pH change resulting in assembly of a self-supporting gel that redissolves when the pH spontaneously increases (# 87 in Fig. 2a and Fig. 3). Control over the pH is realized via two simultaneous reactions: i) hydrolysis of urea by urease, releasing ammonia that increases the pH above the monomer pK_a causing gelation, ii) hydrolysis of methyl formate producing formic acid that decreases the pH. By varying the amounts

of urea, urease and methyl formate, the authors find a mode where the rate of pH increase is much faster than that of pH decrease. In this system, an estimated 76% of the gelator is activated, leading to stiff gels (see section 6 of the SI). The lifetime of the gels can be significantly prolonged by increasing the gelator concentration while maintaining the same amounts of urea, urease and methyl formate. Upon refueling, the onset of gelation is delayed and the lifetime decreased due to waste accumulation, a common issue[82] in chemically fueled systems.

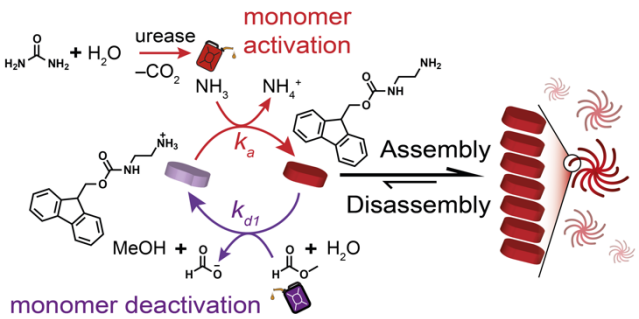

Figure 3 | Regime I, uncoupled: a system of Adams and co-workers[87] with a gelator that follows transient pH change.

Adams and co-workers revisited this system for a different cycle[88], namely a gel–sol–gel instead of a sol–gel–sol transition, which is of use in hydrogel annealing (# 88 in Fig. 2a). After fast activation of a dipeptide-based hydrogelator (pH increase corresponding to dissolution of gel), slower deactivation results in the recovery of the initial gel. The stiffness and morphology of the final hydrogel was shown to be dependent on the deactivation rate. Slower reaction kinetics resulted in a uniform and dense fibrillar network, whereas the initial gel contained mostly spherulites. We cannot exclude the presence of [Assembly]→[Reaction] coupling due to the slower diffusion of the fuel into the initial gel, compared to the activation on the dissolved hydrogelator.

Panzarasa *et al.* reported a transient system[89,90] based on a perylenediimide derivative coupled to a programmable pH cycle (# 89 in Fig. 2a). The latter is obtained from the change in pH (from 5.5 to 10.5) generated by the methylene glycol–sulfite clock reaction. The mechanism

relies on the reaction between formaldehyde and sulfite to produce hydroxymethanesulfonate and hydroxyl ions. Interestingly, by coupling the pH change with the hydrolysis of 1,3-propanesultone or δ-gluconolactone, they could achieve a transient pH change that could be refueled 10 times. The pH change resulted in aggregation of the perylenediimide derivative above its pK_a (6.5) due to π–π stacking and hydrophobic effects. Larger aggregates were formed during stirring, which eventually led to precipitation. Upon hydrolysis of the sultone, the pH decreased to 4.5 causing protonation of tertiary amine groups of the perylenediimide derivative leading to immediate disassembly due to electrostatic repulsion.

Recently, George and co-workers published a detailed study[91] of supramolecular polymerization controlled by the presence of fuels (# 91 in Fig. 2a). Self-assembly of a charge-transfer complex, consisting of tetrapotassium coronene and methyl viologen modified by benzaldehyde, occurs after imine bond formation with 87% conversion. The cooperative mechanism and living character of polymerization were confirmed by seeding experiments. The kinetics of polymer growth was controlled by varying the amine ligands, their concentration and pH, all of which affect the rate of imine formation and hence the self-assembly process. Slow ester hydrolysis was used to trigger disassembly: in first instance by decreasing the pH and thus favoring imine degradation, and later by shortening the amine tail which affects the monomer hydrophobicity and hence the polymer stability. Although we attributed this system to uncoupled examples, the authors also explored enzymatic deactivation using a lipase, where it is unclear whether the self-assembly increases the deactivation rate due to multivalency (i.e., many cleavable bonds in close proximity).

Regime II.

In regime II, deactivation is faster than activation, but high levels of activation (a / c_{tot}) are still achieved due to sufficiently high fuel equivalents. Here, we find the system by Sorrenti *et al.*[92] using an enzymatic reaction cycle that works on a perylenediimide substrate (# 92 in Fig. 2a). The latter has two peptide 'arms' with a peptide sequence LRRASLG that is recognized by a kinase (that phosphorylates the serine residues fueled by ATP) and a phosphatase (that dephosphorylates the serines again). The phosphorylation enhances the self-assembly of the substrate and leads to an inversion of the supramolecular chirality of the resulting supramolecular polymer. Upon dephosphorylation, the original substrate and assemblies are recovered. When both enzymes and a shot of ATP fuel are added to the same batch reaction, transient self-assembly was observed.

Besenius and co-workers showed a unique example[93] of a transient system where both stimuli, responsible for assembling and disassembling of a monomer, are introduced by the same reaction (# 93 in Fig. 2a and Fig. 4). Oxidation of glucose catalyzed by glucose oxidase produces gluconolactone and hydrogen peroxide. Gluconolactone hydrolyses to produce gluconic acid, thus lowering the pH and leading to protonation and self-assembly of the monomer, yielding 99.8% activation. Concurrent oxidation of methionine residues in the monomer—due to increasing amounts of hydrogen peroxide—reintroduces charge repulsion and causes disassembly. Looking in detail at Figure 3 of their paper, one might notice that increased amounts of glucose oxidase (i.e. increasing the amounts of both fuels) results in longer gel lifetimes and slower deactivation and disassembly processes. This observation may suggest that the deactivation and disassembly are coupled (see sections on coupled systems below), but this remains to be confirmed.

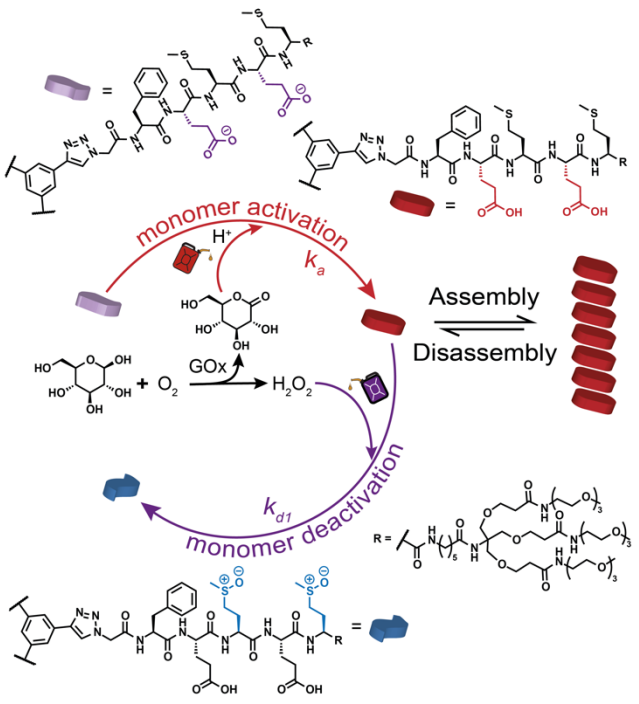

Figure 4 | Regime II, uncoupled: an example from Besenius and co-workers[93] with transient self-assembly driven by activation via pH change and by de-activation via oxidation. Note that two different types of deactivated monomers exist (purple and blue).

Regime III.

In regime III, levels of activation are low as compared to regimes I and II since the fuel concentration is low, and the activation process is slower than that of deactivation. As self-assembly is more challenging with small amounts of activated monomer, there are very few examples of transient activation in this regime. Quintard and co-workers introduced a system[94] that performs a sol–gel–sol transition (# 94 in Fig. 2a). They start off with a solution of the anionic CO_2-adduct of O-*tert*-butyl-L-tyrosine (i.e., the carbamate form), with protonated DBU base as the countercation. Addition of trichloroacetic acid (TCA) leads to decarboxylation and (via an intermediary protonated species to) the formation of neutral O-*tert*-butyl-L-tyrosine, which forms

a chiral organogel. By reabsorbing CO_2, the initial carbamate is restored, and the gel disappears. Interestingly, the base DBU acts as a catalyst since it is not getting used up throughout the cycle, and it aids in both the activation (promoting decomposition of TCA into CO_2 and chloroform) and deactivation (as a counter-ion for the anionic carbamate). At the same time, it seems not to influence the self-assembly process. Due to the convenient waste removal of gaseous CO_2 and volatile chloroform, the system was shown to go through 25 refueling cycles with very little damping. We assigned the system to regime II because we include both decarboxylation and intermediate protonation in the activation process, which when combined are slower than deactivation.

In 2018, the group of George[95,96] presented ATP-fueled supramolecular polymerization of dipicolylethylenediamine–zinc (DPA–Zn) containing monomers (# 95 in Fig. 2a and Fig. 5). In the absence of fuel, the monomer exists in a pre-assembled slip-stacked state. Multivalent binding of ATP to several DPA-Zn monomers induced a left-handed helical motif in the supramolecular polymer, giving a maximum activation of about 7%. The authors introduced the potato apyrase enzyme that catalyzes the hydrolysis of ATP, thereby leading to depolymerization. The enzymatic activity is shown to be non-selective to unbound ADP present simultaneously with bound ATP, which suggests that self-assembly does not likely influence the kinetics of the deactivation process—i.e., the system is uncoupled.

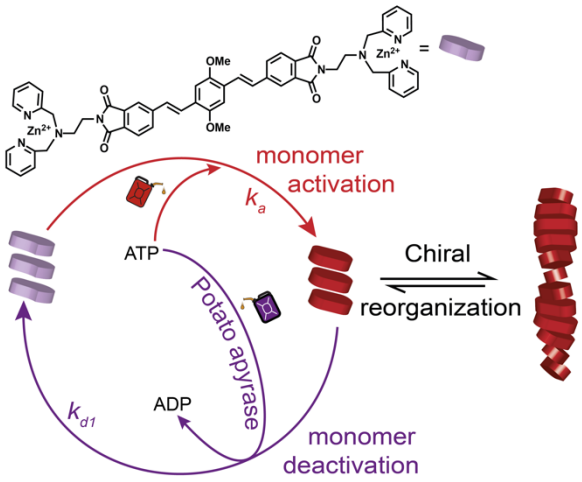

Figure 5 | Regime III, uncoupled: a system of George and co-workers[95] transient chiral reorganization of pre-assembled monomers triggered by interaction with ATP.

Regime IV.

Up to now, we have not found uncoupled systems that are in regime IV (Fig. 2a), which combines fast activation with low fuel equivalents. We can see from the model that sparse fuel would lead to low degrees of activation (Fig. 2d), which would further decrease when pushing deeper into the regime (i.e., more negative x and y values in Fig. 2a). Consequently, this regime is unfavorable for achieving transient self-assembly unless the assembling molecule has a very low critical aggregation concentration, where even low activation (e.g., a / c_{tot} < 0.05) would result in significant assembly or gelation. As we will see below (section 3.2), coupling the reaction cycle to self-assembly (and thus protecting from deactivation) can be helpful in promoting transient assembly under otherwise unfavorable conditions like those in regime III or IV.

2.3 Other strategies to obtain transient self-assembly

There are a few other strategies that also lead to transient self-assembly that are not just due to the ratio of deactivation/activation and fuel concentration present in the system, as we have described

earlier in this section. Below we describe three interesting systems where other effects come into play.

Reduced activation and deactivation by monomers and assemblies. In 2015 Walther and co-workers[19] used the enzyme urease to convert urea into CO_2 and NH_3, thus slowly increasing the solution pH (# 19 in Fig. 2a). Adding urea-containing acidic buffer solution to a urease solution at pH 9.5 resulted in a transient high–low–high pH cycle. Combining this with a pH-responsive peptide hydrogelator (Fmoc-LG-OH) resulted in transient gelation where self-assembly follows the change of pH. Assuming absence of co-assembly between charged and neutral peptides we estimate the degree of activation to be 94% (see section 6 of the SI). Interestingly, the pH time-progression was significantly slower in presence than in absence of the peptide, affecting both the activation and deactivation phase. Since the peptides can be protonated, they increase the buffer capacity of the overall system (in addition to the available citrate buffer). This makes it harder to return to the high pH state due to the urea-urease reaction. The authors observed this effect because of the almost equimolar amounts of peptide and buffer molecules, whereas usually the buffer is in large excess. In this system, it is the chemical nature of the monomer (i.e., it contains a carboxylic acid) that influences the activation and deactivation reactions. The work of Mondal et al. on a related system showed a similar behavior when using 1 M HCl instead of an acidic buffer.[97]

Influence of mass transport phenomena. There are systems where transient self-assembly was achieved, but through the interaction with mass transport. For example, control of pH was implemented by Miravet and co-workers[98] via yeast catalyzed hydrolysis of sucrose that gradually produces CO_2 *in situ* causing acidification of the medium. Protonation of carboxylic acid groups in amphiphilic monomers triggers their assembly into fibrillar networks. Depletion of CO_2 by

exchange with the surrounding air in the system over time increases the pH above the monomer pK_a resulting in dissolution of gel due to charge-charge repulsion.

Recently, the group of Kim[99] investigated a transient self-assembly controlled by acid–base fuels, where the transient formation of microstructures can be tuned by the ratio of acid and base in the solution. Particularly, they used a non-aggregating monomer (methyl orange) that is activated under acidic conditions. The activated monomer forms aggregated microcrystals due to electrostatic attraction. Next, CO_2 absorption into the solution lowered the pH leading to monomer protonation and consequent crystallization.

It is clear that buffering effects or mass transport phenomena can play a key role in transient self-assembly, but for the sake of simplicity we will not take this into consideration in our analytical models.

3. Coupled Transient Self-assembly

3.1 Model

According to the Transient Activation model (eq. 1–2), it is difficult to activate appreciable amounts of monomer (i.e., high a / c_{tot}) in regimes III or IV, and thus high monomer concentrations and/or strong monomer–monomer interactions would be required to surpass the critical aggregation concentration. However, as we show in this section, coupling chemical reactions to self-assembly can alter these conclusions, thereby enabling transient self-assembly under otherwise unfavorable conditions. In contrast to the Transient Activation model (section 2.1), we now consider that the rates of deactivation can differ for monomers in solution as compared to those in a polymer. We will focus our discussion on systems in regime III, which are most unlikely to achieve efficient transient self-assembly in the absence of [Assembly]→[Reaction] coupling; however, the model we developed applies to all regimes.

To describe the influence of self-assembly on monomer activation/deactivation, we consider an isodesmic supramolecular polymer that assembles and disassembles by reversible reactions of the form

$$A_i + A_j \overset{k_{\pm}}{\longleftrightarrow} A_{ij}$$

with forward rate constant k_+ and backward rate constant k_-, which are assumed independent of polymer length i, j, $i+j$. The thermodynamics and kinetics of this idealized model are well known as reviewed in Section 1 of the SI. Starting from activated monomer, the (number) concentration $a_n(t)$ of polymers of exactly length n follows an exponential distribution that evolves monotonically in time towards equilibrium (see Figure S1 in the SI). The features of this transient distribution are conveniently summarized in terms of the first two moments: $m_0(t) = \sum_{n=1}^{\infty} a_n(t)$, the total (number) concentration of polymers of any length; and $m_1(t) = \sum_{n=1}^{\infty} n\, a_n(t)$, the total concentration of activated monomers. Importantly, isodesmic polymerization can be described exactly in terms of the dynamics of these moments without reference to higher order moments (e.g., dispersity) or approximation schemes. Consequently, this model provides a convenient framework with which to explore the coupling of supramolecular self-assembly and chemical activation described by our 'Coupled Isodesmic Transient Self-assembly' model (see SI section 4). In this idealized description, only the activated monomer can form polymers, whereas the deactivated monomer stays disassembled. Once an activated monomer is inside the polymer, it deactivates with a rate constant k_{d2} that differs from that in solution k_{d1}. In addition to the concentrations of fuel f and activated monomer a_1, the state of system is characterized also by the partial moments $m_0' = m_0 - a_1$ and $m_1' = m_1 - a_1$, which describe the concentrations of polymer and polymerized monomer, respectively, without the monomer contribution. The time evolution of these concentrations is governed by the following differential equations

$$\dot{f} = -k_a f\left(c_{tot} - a_1 - m_1'\right) \tag{3}$$

$$\dot{a_1} = k_a f\left(c_{tot} - a_1 - m_1'\right) - k_{d1}' a_1 + 2k_{d2}' m_0' - 2k_+ a_1\left(a_1 + m_0'\right) + 2k_- m_0' \tag{4}$$

$$\dot{m_0'} = k_{d2}'\left(m_1' - 4m_0'\right) + k_+\left(a_1^2 - m_0'^2\right) + k_-\left(m_1' - 3m_0'\right) \tag{5}$$

$$\dot{m_1'} = -k_{d2}'\left(m_1' + 2m_0'\right) + 2k_+ a_1\left(a_1 + m_0'\right) - 2k_- m_0' \tag{6}$$

Here, c_{tot} is the total monomer concentration, k_a is the rate constant for (chemical) activation, k_{d1}' and k_{d2}' are the pseudo-first-order rate constants for (chemical) deactivation, k_+ is the assembly rate constant, and k_- is the disassembly rate constant. We use the partial moments m_0' and m_1', including contributions from all polymers of length 2 or greater, to more clearly distinguish the dynamics of the polymer from that of the activated monomer.

We now re-evaluate regime III of the (uncoupled) Transient Activation model, where the only difference is the coupling of self-assembly to the activation/deactivation. We will discuss two different scenarios: 1) that of 'catalysis', when deactivation is accelerated by on-polymer catalysis; and 2) that of 'shielding', where monomers are protected from deactivation once assembled. As we will see later in the literature examples, there are cases where deactivation (by hydrolysis) is accelerated due to catalytic activity from proximal monomers in the supramolecular polymer structure. This means that k_{d2} is much larger than k_{d1} in our model. The result is that monomer activation is much more pronounced (compare the solid to the dashed line in Fig. 6a), and self-assembly can occur. At the same time, when self-assembly (of dimers or larger) occurs it results in rapid deactivation and disassembly. Effectively, a very narrow distribution of dimers is present through the transient cycle (Fig. 6b).

The second, more common scenario is when monomers can no longer be deactivated once self-assembled into supramolecular polymers, resulting in a shielding effect. To illustrate this effect, we consider an isodesmic polymer with an equilibrium length of 20 (i.e., $k_+ c_{tot}/k_- = 400$)

that assembles much faster than the rate of deactivation (i.e., $k_+/k_a = 900$). Shielding in this case means that deactivation cannot occur in the polymerized state such that $k_{d2} = 0$. In Fig. 6c we see that the fraction of (activated and subsequently) assembled monomers is ~0.5, more than an order of magnitude higher than for the uncoupled case (dashed line, identical to Fig. 2e). Along with monomer activation, the polymer develops a distribution that peaks at an average length of 16 (Fig. 6d). In simpler words, the self-assembly protects the activated monomers from deactivation in solution. Under such conditions—even if the deactivation is much faster than the activation regime and fuel is not in great excess—there can still be a large amount of self-assembled species.

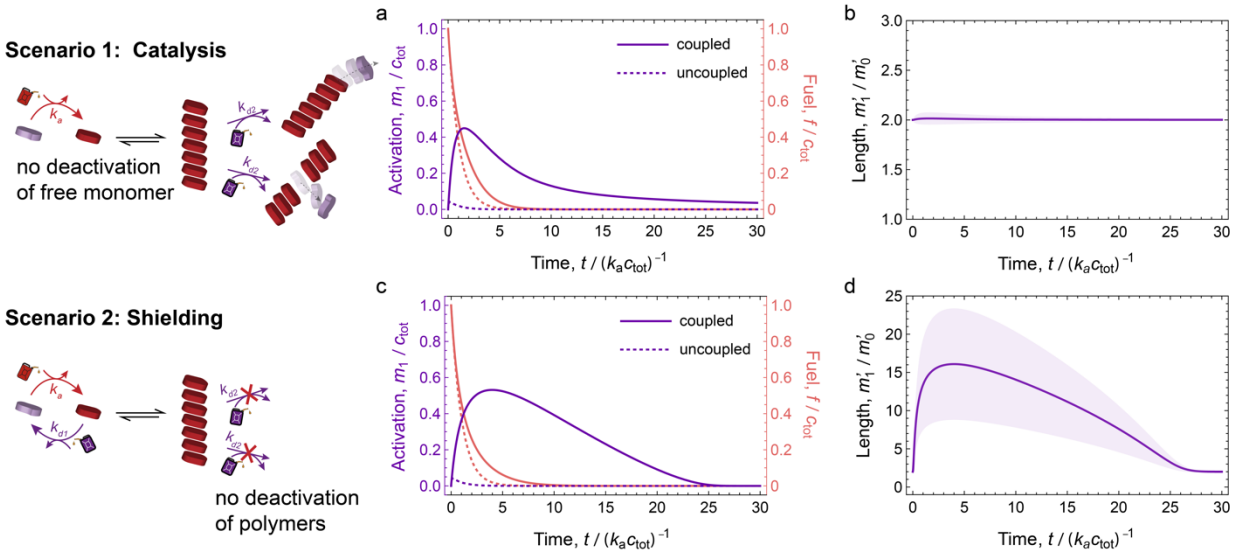

Figure 6 | Transient self-assembly coupled to isodesmic polymerization for two scenarios: 1) catalysis and 2) shielding. a) degree of activation versus time, comparing the uncoupled (section 2) and coupled model (section 3). b) average polymer length (and distribution in the shaded area). c,d) the same as panels a and b, but for scenario 2. In this model we consider $k_{d2} = k_{d3}$ (this will be different in section 4).

We turn now to examples where [Assembly]→[Reaction] coupling between (dis)assembly and (de)activation is evident or suspected. We will not differentiate between isodesmic or

cooperative mechanisms of polymerization since often they are not specified or studied. The literature examples are mapped onto the same Transient Activation model using the apparent activation and deactivation rates since most authors did not measure the chemical- and/or self-assembly kinetics separately. See SI section 6 for a detailed description of how these apparent kinetic parameters were estimated.

3.2 Literature examples

Scenario 1: Catalytic deactivation upon self-assembly ($k'_{d2} \gg k'_{d1}$). In 2018 (# 81 in Fig. 2a), Das and co-workers introduced a transient self-assembly system[81] based on an amphiphilic molecule containing histidine. In the presence of the activating fuel EDC (1-Ethyl-3-(3-dimethylaminopropyl)carbodiimide), the substrate self-assembles due to the formation of an ester bond with 4-nitrophenol, leading to a self-supporting gel within 2 minutes. With time, the gel breaks and the initial solution is recovered. The transient behavior can be explained due to the histidines, which greatly accelerate the hydrolytic deactivation of the ester when in close proximity to each other inside the self-assembled structures. Interestingly, by using phenol, instead of a nitrophenol, they increased the gel lifetime from hours to about 5 days. The increased hydrophobicity of the phenol derivative protects the supramolecular polymers from deactivation. The same principle was used by the group to show transient amyloid polymerization and probe the electrical properties of the system.

In 2019 (# 100 in Fig. 2a), the same group described transient metastable helical nanostructures based on the previous system. In this work[100], the self-assembly was driven by a stearoyl histidine and a nitrophenyl ester of a stearoyl phenylalanine. The latter is prone to co-assemble due to the carbon tail and the phenyl ring, leading to the formation of a gel in about 2h.

No activating chemical fuel is consumed. Again, the cooperative effect of proximal histidines catalyzes the hydrolysis of the ester bond releasing stearoyl phenylalanine and nitrophenol, thus dissolving the gel. The authors observed the formation of helical ribbons after 2h, and 90% of the population featuring helical morphology after 4h. After 6h, the population of helices started to decrease, corresponding to the point where 15% of the ester bonds were hydrolyzed. And after 10h, all helical nanostructures disappeared.

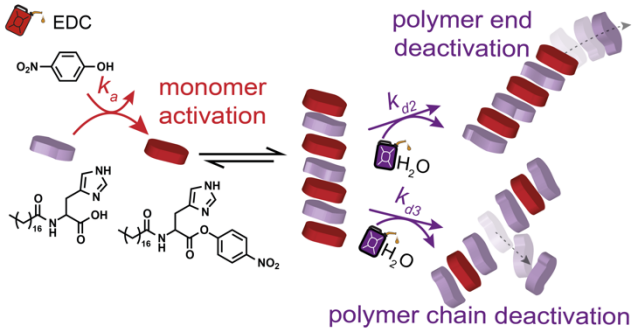

Figure 7 | Catalytic deactivation, close proximity of histidines accelerates hydrolysis.[81]

Scenario 2: Self-assembly shields molecules from deactivation ($k'_{d2} \ll k'_{d1}$). Ulijn and co-workers studied in 2015 a transient tripeptide system[101] where a DF dipeptide was extended by either F, Y, W, L, V, S, or T using chymotrypsin-catalyzed transacylation (# 101 in Fig. 2a). Only for extensions by F and Y did tripeptide formation—i.e., DFF and DFY—lead to supramolecular polymerization and gelation. Whereas, the forward rates of F and Y adding onto DF were similar (92% conversion within 30 minutes), the backward rates (i.e., hydrolysis from the tripeptide back to the dipeptide) was 8 times slower for DFF than for DFY. It shows that the more hydrophobic DFF tripeptide assemblies shield the activated monomers better from deactivation (due to hydrolysis). Upon refueling, the reaction cycle could be repeated 3 times, with diminishing amounts of tripeptide after each cycle due to waste (DF) accumulation.

Earlier, in 2013 (# 102 in Fig. 2a), the same research group showed a similar transient system[102] based on naphthalene-dipeptide gelators. They started from a naphthalene bearing tyrosine methyl ester Nap-Y-OMe that could be extended with tyrosine amide, phenylalanine amide, or leucine amide by catalyzed transacylation. The respective products, Nap-YY-NH_2, Nap-YF-NH_2 and Nap-YL-NH_2 can self-assemble into hydrogels, but over time slowly hydrolyze to their corresponding acids (Nap-YX-OH). They pointed out that the sol–gel–sol conversion in transient systems is only observed if the peak activated monomer concentration exceeds the critical gelation concentration. A quantification of the gel properties by rheology showed that the highest stiffness gel Nap-YF-NH_2 also had the slowest hydrolysis/disassembly rates. This shows that the deactivation and self-assembly processes are clearly coupled.

Finally, in 2018 Ulijn and co-workers used their approach to achieve transient supramolecular chirality and conductivity in a naphthalenediimide-peptide system[103] (# 103 in Fig. 2a). Alpha-chymotrypsin again catalyzes amide bond-formation and hydrolysis of tyrosine methyl ester that were attached to both sides of the naphthalenediimide. Interestingly, the chirality of the tyrosine is of key importance: reactions on L-tyrosine proceed in hours, whereas those on D-tyrosine need weeks. This unique property allowed the authors to obtain time-control over which monomer is activated first, and which one later on. As a result, left-handed chiral nanofibers formed after hours and were slowly outcompeted by right-handed nanotubular structures after 2 weeks. In addition, transient assembly from sheets to one-dimensional fibers led to time-dependent conductance in an electrical circuit.

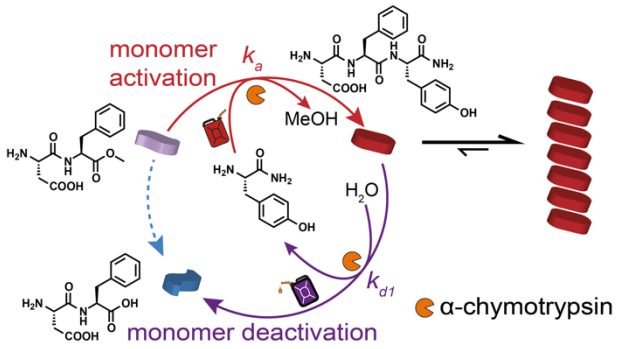

Figure 8 | Self-assembly shields monomers from deactivation.[101]

Recently, Singh et al. developed a new reaction cycle[104] where they achieved temporal control over a gel–sol–gel conversion (# 104 in Fig. 2a). The activated monomer is an aldehyde-bearing saccharide hydrogelator, which can be deactivated by reaction with dithionite, leading to its hydroxy sulfonate analog and disassembly. Reaction of the hydroxy-sulfonate with formaldehyde can restore the aldehyde group and again activate self-assembly. However, dithionite and formaldehyde react very fast with one another, so a time-delayed release of formaldehyde was needed. To this end, the authors used the slow ring-opening of δ-gluconolactone (GdL), which gradually decreases the solution pH, enabling in turn the acid-catalyzed conversion of hexamethylenetetramine to formaldehyde. Hexamethylenetetramine is effectively a 'pre-fuel', from which the fuel (formaldehyde) is formed slowly. GdL provides a throttle for the pre-fuel conversion. As such, at higher GdL concentrations the authors observed a fast gel–sol–gel conversion whereas at lower GdL concentrations, the sol state was maintained for much longer. In more recent work[105], the authors looked at three chemically similar gelators, and showed that self-assembly into fibers can shield monomers from deactivation (by dithionite).

Boekhoven and co-workers[14] (# 14 in Fig. 2a) noticed a strong shielding from hydrolysis in presence of supramolecular self-assemblies. In their system, Fmoc-protected amino acids (or tripeptides) undergo activation and hydrogelation upon conversion into their anhydride analogs.

The more anhydride produced, the stiffer the gel and the lower the hydrolysis rate. The authors observed that the (hydrolytic) deactivation rate was two orders of magnitude lower for strongly assembled molecules as compared to non-assembling or weakly assembling anhydrides. The coupling between deactivation and assembly was approximated in their kinetic model by introducing a second *k*-value for hydrolysis above a threshold concentration of activated monomer. The approach was expanded by the group in later works to obtain different transient materials.[106–113]

The same group later studied how the molecular structure of a (peptide) monomer, the ionic strength of the solution, and the amount of added fuel (EDC) dictate whether self-assembly is transient, permanent, or altogether absent.[114] Going from the deactivated (diacid) to activated (dianhydride) monomer reduces the number of charges by 2. Depending on the balance of attractive and repulsive interactions encoded in the molecular design and due to the solution conditions (ionic strength and pH), the following scenarios are found: i) activation leads to assembly, and deactivation to disassembly, ii) activation results in irreversible assemblies that are not prone to deactivate by hydrolysis, iii) activation does not shift the charge balance to attractive sufficiently, so no assembly is observed.

Thordarson and co-workers[115] (# 115 in Fig. 2a) showed a system where acidification of an aqueous solution of dianionic *N,N'*-dibenzoyl-L-cystine (DBC^{2-}) leads to protonation to DBC and gelation (at pH 2.7, 88% of DBC is activated). Deactivation occurs by splitting the disulfide bond at the center of DBC by TCEP reduction. Though TCEP reduction has been shown to be pH-independent, the authors observed that the deactivation was ~5 times slower at pH 2.7 as compared to pH 3.1. At the lower pH, more of the DBC was self-assembled, thereby shielding the molecules from deactivation by TCEP reduction. Based on kinetic measurements the authors argue that the

dissociation of DBC from the self-assembled structures into solution (where it can be reduced efficiently) is the rate limiting step.

Similarly, Guan and co-workers (# 116 in Fig. 2) developed a reaction cycle[116] based on thiol-disulfide oxidation-reduction reactions using *N*-benzoyl-cysteine amide. Upon oxidation by hydrogen peroxide, *N,N'*-dibenzoyl-L-cystine amide forms with 44% conversion and rapidly assembles into a self-supporting gel. Over time, the molecule is deactivated because of disulfide reduction by dithiothreitol to form deactivated monomer (*N*-benzoyl-cysteine). Compared to the Thordarson system, here the monomer can be fully recovered to perform further reaction cycles upon injection of additional aliquots of fuel. It reduces the production of waste products, since the initial deactivated monomer can be reformed. The ability to activate and deactivate monomers repeatedly is potentially important for materials applications, which would otherwise lose their structure after just one cycle (of activation/deactivation). By comparing the apparent deactivation rate constant with that of analogous literature reactions and considering the similarity with the monomer of Thordarson, we suspect that this system also exhibits coupling between deactivation and assembly (see more details in SI section 6).

Looking back at the very first example of chemically fueled supramolecular polymer by van Esch and co-workers,[6,117] one finds interesting dynamical behaviors that derive from the complex interplay between reaction and assembly (# 6, 117 in Fig. 2a). Methylation reactions on anionic *N,N'*-dibenzoyl-L-cystine DBC^{2-} (partially) neutralize the negative charges of the carboxylate groups (to DBC^{-}) resulting in self-assembly of the molecule into fibers and macroscopic gelation. Over time, the molecule hydrolyzes back to DBC^{2-}, and the fibers and gel disappear. Interestingly, the gel state persists well after depletion of active monomer. As they disassemble, fibers were observed to collapse suddenly rather than shrink gradually, and at certain times, both growing and shrinking fibers were observed under common conditions. These findings

support the hypothesis that hydrolysis occurs inside the fibers but that disassembly does not occur until a threshold number of negative charges is reached. This coupling between the kinetics of deactivation and disassembly and the resulting dynamics are what make this system so interesting, and why it has inspired others to advance the field.

Towards mechanical functions. Having discussed the different ways to obtain transient self-assembly of either uncoupled or coupled systems (sections 2 and 3, respectively), we would like to highlight a final example moving towards a bio-inspired function. Mechanical work is carried out by natural chemically fueled polymers like actin filaments[118] and microtubules[119–121] that exert forces onto the cell wall, for example. The mechanical work in the latter cases has been quantified in detail. In contrast, for artificial systems the focus has been on getting the reaction cycles to work, i.e., in achieving transient self-assembly, but not so much on quantifying the mechanical work that could possibly be exerted. The group of Hamachi, however, has recently demonstrated force generation in a propagating wave of supramolecular fibers[122] whose growth and degradation are spatiotemporally controlled by non-interfering chemical stimuli. To demonstrate such behavior, a solution of a peptide hydrogelator together with a catalyst was prepared between two glass slides. Simultaneous addition of both activating and deactivating fuels at one edge of the system led to a travelling front of transient nanofiber assembly that propagated across the solution as the fuels advanced by diffusion. The amount of fibrous material, its lifetime and movement across the sample were shown to be highly dependent on reactant ratios. The authors quantitatively compared the generated force in their system to that of biological examples by measuring the speed of bead displacements along the path of the gelation wave. Although the persistence length of their fibers was akin to that of actin, the generated force was 150–550 times weaker than the stalling force of actin and microtubule polymerization. This observation was explained by the lack of directionality

in artificial fibers and their stochastic entanglement compared to those in nature. The work, however, demonstrates biological-like force generation and serves as inspiration for future work on dissipative self-assembling materials.

4. Oscillations in coupled cooperative supramolecular polymerization

4.1 Prelude

As mentioned in the introduction, microtubules are fascinating structures that can reproduce biological functions *in vitro* such as force generation, active transport, and centrosome centering. Another interesting finding is that depolymerization ('catastrophes') and polymerization ('rescues') can be synchronized across large sample volumes, thereby enabling temporal oscillations in the number and size of supramolecular assemblies. This behavior was first observed in the 1980s by heating tubulin heterodimers together with an excess of GTP to 37 degrees, while monitoring the assembled structures by X-ray scattering.[123,124] These experiments revealed damped oscillations in scattering intensity—and thus microtubule length and concentration—for ~20 minutes.

A glimpse of oscillations in an artificial supramolecular polymer system can be found in the PhD thesis of Cantekin[125], where the self-assembly of a thio-BTA (benzene-1,3,5-trithioamide derivative bearing (S)-3,7-dimethyloctyl side chains) was studied. The thio-BTA assembles in methylcyclohexane through a cooperative polymerization mechanism,[126] though with a lower 'cooperativity factor'[127] than that of its (amide-)BTA analog. At room temperature and mM monomer concentrations, the resulting polymers show supramolecular chirality and a degree of polymerization of ~1500 monomers. The NH-protons of the thio-BTA—needed for intermolecular hydrogen bonding between stacked monomers—can be abstracted using an organic base (DBU: 1,8-diazabicylcoundec-7-ene, pK_a = 12). After a slow heating–cooling cycle in presence of one

equivalent of DBU per thio-BTA, the circular dichroism signal was reduced by 30–50%, and the length decreased by 15%. The latter indicates that both the supramolecular chirality as well as the assembly are influenced by DBU. Upon rapid quenching from 80 °C to 20 °C , damped oscillations were observed in the circular dichroism as well as the UV-visible spectra (Figure 9). Though it is unclear whether the spectroscopically observed oscillations also affect the size of the assemblies, a couple of key ingredients can be discerned: i) the assembly of the supramolecular polymer is cooperative, that is, undergoing nucleation and elongation; ii) there is a process that can deactivate the monomer (i.e., deprotonation). Below, we will see how these two ingredients are important in obtaining supramolecular oscillations. The Cantekin system has other complications that require further study, for example, the pK_a of the base and monomer may depend on temperature[128] and on the local environment within the assembly.

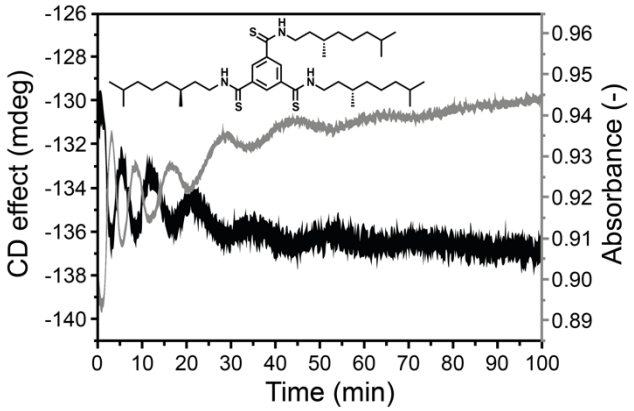

Figure 9 | Damped oscillations in circular dichroism and absorbance in a quickly cooled supramolecular polymer system.[125]

In general, it is difficult to find oscillations in any system if one is not keeping the 'control parameter' (in our case the fuel concentration) at a constant level, that is, if we are not working under (dissipative) non-equilibrium steady state (NESS) conditions. Only a few systems show many oscillations under batch conditions, whereas many oscillate in continuous stirred tank

reactors.[129] One of the reasons is that oscillations usually only occur in a narrow window of the experimental parameters (i.e., a small region in the 'phase space'). When working in batch, the conditions are only constant for a short period of time. Even when maintaining steady state conditions, it might take time for the system to relax to the NESS.[130] In dissipative self-assembly examples, NESS conditions are still very rare. One system was demonstrated by Sorrenti *et al.* by the use of a continuous flow device.[92] The system was confined by a dialysis membrane where fuel was continually supplied and waste removed. The authors showed different non-equilibrium steady states at various (steady state) fuel concentrations. More recently, Heinen *et al.* showed (pseudo-)steady state conditions in a DNA-based system.[131] The lifetime of the self-assembled supramolecular polymer strictly depends on the fuel consumption, resulting in steady state of a few hours up to a week long, with increasing fuel concentration.

4.2 Model

We generalize a recent model[132] that was used to describe damped oscillations in the number and size of supramolecular polymers based on perylenediimide monomers. In that system, charge-neutral monomers self-assemble through a cooperative mechanism based on nucleation and elongation. Monomers are deactivated by chemical reduction, leading to a charged dianion that rapidly disassembles. The deactivated monomer can be activated again by oxidation in solution. The resulting cycle of assembly, deactivation, disassembly, and activation is maintained by a steady delivery of activating and deactivating chemical fuels (i.e., oxidant and reductant, respectively). For simplicity, the original model considered deactivation only at the polymer ends and not in solution nor at positions along the polymer chains. The model revealed damped oscillations in the number and size of polymer assemblies; however, a full exploration of the parameter space was limited by the simplifying assumptions made.

In the current model, we consider all processes that can reasonably occur, including various types of polymer assembly and disassembly as well as chemical activation and deactivation (Fig. 10a). The relevant assembly processes describe the nucleation, elongation, and coagulation of polymer chains. The reverse disassembly processes of de-nucleation, de-elongation, and de-coagulation (i.e., fragmentation) are included in a thermodynamically consistent manner. We assume a common rate constant k_+ for all assembly processes, which are approximated as diffusion limited. The rate constants k_{ij}^- for the reverse disassembly processes depend on the sizes i and j of the resulting products as described by a simple model of cooperative polymerization (see SI section 1.4). For a critical nucleus size $n_c = 2$, we distinguish three rate constants for disassembly: de-nucleation of the dimer $K_c k_+$, de-elongation of polymers by monomer detachment $K k_+$, and de-coagulation (fragmentation) of polymers by polymer detachment $K^2 k_+ / K_c$. To describe the coupling between self-assembly and chemical deactivation, we distinguish three pseudo-first order rate constants of deactivation for different monomer environments: free monomer k'_{d1}, polymer ends k'_{d2}, and polymer chain k'_{d3} (see Fig. 10a). We assume that monomer deactivation within polymer chains leads to their rapid fragmentation; stable polymers include monomers of a single type. The resulting model is fully specified by eight parameters: the rate constants for assembly k_+, activation k_a, and deactivation k'_{d1-3}; the dissociation constants K and K_c for de-nucleation and de-elongation; and total monomer concentration c_{tot}.

A detailed treatment of these different mechanisms requires the numerical solution of many rate equations—one for each polymer length considered (typically < 1000 to limit computational costs). These solutions describe the time evolution of the different species concentrations—namely, deactivated monomer $d(t)$, activated monomer $a_1(t)$, and activated polymer $a_n(t)$ of length $n = 2, \ldots, n_{max}$. As in section 3.1, the transient polymer size distribution can be summarized in terms

of its moments—namely, the total concentration of polymer chains $m_0'(t)$, and the total concentration of polymerized monomer $m_1'(t)$ (both excluding free monomer). Importantly, by solving the kinetic rate equations numerically for all polymer lengths, one can explore the model parameter space more fully in search of oscillatory dynamics without limitations due to simplifying assumptions or approximations.

4.3 Identifying and understanding supramolecular oscillations

Using optimized methods to integrate large numbers of coupled ODEs (see SI, section 2.2), we performed a 'brute force' numerical search of the model parameter space in pursuit of oscillatory behaviors. As shown in Figures S9 and S10, we identified a single parameter region that supports sustained oscillations. Several useful lessons can be learned from the conditions identified:

i) the total monomer concentration should be more than 10^4 times higher than the dissociation constant for elongation ($c_{tot}/K > 10^4$); one should work at 'high' concentrations. For a typical value of $K = 10^{-6}$ M, monomer concentrations greater than 10 mM are required; however, stronger assemblers with smaller K could oscillate at lower concentrations.

ii) polymerization should be highly cooperative[127] such that elongation is much more favorable than nucleation or, equivalently, the dissociation constant for nucleation is much greater than that of elongation ($K_c \gg K$).

iii) the rate constant of 'end deactivation' should be fast as to compete with polymer elongation ($k_{d2}' \sim k_+ c_{tot}$); polymers are dynamically maintained by the balance of two independent kinetic processes.

iv) the rate constant of 'chain deactivation' should be slow relative to that of 'end deactivation' ($k_{d3}' \ll k_{d2}'$). This condition is not implausible considering that many one-dimensional

polymers further assemble into bundles, thereby inhibiting the deactivation of interior monomers.

v) the rate constant of monomer activation in solution should be faster than that of deactivation but slower than that of disassembly ($k'_{d1} < k_a < k_+ K$). Faster deactivation leads to complete disassembly.

These conditions highlight the challenge of realizing oscillatory dynamics in practice due to the careful tuning of multiple rate processes required. In particular, the present model requires *both* catalysis and shielding (section 2.2): deactivation of polymer ends must be faster than that of free monomer (catalysis); meanwhile monomer deactivation in polymer chains must be comparatively slow (shielding).

Figure 10b shows a typical solution within the oscillating regime. During each cycle, the concentration of activated monomer (red) rises steadily at the expensive of the deactivated monomer (purple). When the concentration of activated monomer exceeds a critical value, it triggers autocatalytic growth in the concentration of polymerized monomer (black, m'_1) followed by rapid depletion of activated monomer and deactivation-induced disassembly. To better understand the mechanisms underlying these oscillations, we examined how the different processes (e.g., elongation, chain deactivation, etc.) contribute to changes in the polymer moments m'_0 and m'_1 over the course of an oscillation cycle (see section 5.2 of the SI for details).

The key findings are captured in Figure 10c, where we plot the time rate of change in the polymer moments highlighting the dominant processes involved. Inspection of m'_1—the polymerized monomer concentration—reveals a continuous 'tug-of-war' between elongation working to make polymers longer and chemically fueled end deactivation working to shorten them (Fig. 10c, top). Above a critical concentration of activated monomers, elongation is slightly faster

than end deactivation, thereby driving polymer growth. During this growth phase, both processes increase their rates exponentially with the growing number of polymer chains, which provide sites for elongation and end deactivation. Figure 10c (top) shows how the growing rate of elongation leads that of end deactivation, reaching its peak earlier before being overtaken by end deactivation.

The exponential growth in the number of polymer chains is driven by chain deactivation, which divides polymers in two, creating more sites for elongation (see k_{d3} in panel a). This mechanism is the chemically fueled equivalent of mechanical fragmentation (e.g., due to viscous shear forces), which has been shown to drive exponential growth in the number of growing polymers.[133,134] Figure 10c (bottom) shows how the polymer concentration m_0' rises due to chain deactivation during the growth phase. One can consider chain ends to be catalysts for the assembly of activated monomers. An increase in chain ends accelerates the growth of polymer chains, which can be chemically severed, thus producing even more chain ends. Together, the combination of elongation and chain deactivation drive autocatalytic growth in the number of polymers of a characteristic size. Excitingly, our findings suggest that such autocatalytic growth can be achieved chemically without the need for mechanical forces due to stirring to actively break supramolecular polymers.

Eventually, as autocatalytic polymer growth depletes activated monomer from solution, the monomer concentration falls below a critical value thereby shifting the 'tug-of-war' between elongation and end deactivation in favor of the latter. During this decay phase, the polymer ends continue to catalyze monomer deactivation, thereby driving the concentration of activated monomers even lower. The amount of polymerized monomer gradually decreases by end deactivation (less elongation) as the average polymer length shrinks (Fig. 10c, top). Meanwhile, the number of polymers, once growing by chain deactivation, now decreases due to de-nucleation (Fig. 10c, bottom). Ultimately, the vast majority of polymers are completely disassembled, and the

activated monomer concentration falls well below that required for growth. In the time leading up to the next burst of growth and decay, the concentration of activated monomers rises slowly due to chemical activation.

Critical to the formation of sustained oscillations are time delays associated with both the autocatalytic growth and the transient unraveling of polymer assemblies. Increasing the polymer concentration by many orders of magnitude takes time, during which the concentration of activated monomer continues to rise well beyond the critical value required for growth. Likewise, the shrinking of polymer chains by end deactivation and their removal by de-nucleation takes time, during which the activated monomer concentration falls well below the critical value. These two delay mechanisms prevent the system from reaching a stable steady state, at which the processes of assembly/disassembly and activation/deactivation are balanced.

In addition to their oscillatory dynamics, the polymers formed during each cycle of growth and decay exhibit transient size distributions that differ both quantitatively and qualitatively from their equilibrium form. Not surprisingly, the addition of disassembly mechanisms based on chemical deactivation leads to shorter polymers as compared to the equilibrium length. For the system in Figure 10, the number average polymer length oscillates between 12 and 38 during each cycle—much shorter than its equilibrium length of ca. 10^7. Moreover, the transient size distribution is qualitatively different from the exponential form expected for both equilibrium polymers and dissipative polymers at steady state. During the autocatalytic growth phase, the interplay between polymer growth by elongation (less end deactivation) and division by chain deactivation drives the kinetic selection of the 'fittest' polymer distribution (i.e., that which grows fastest). The growth of this distribution requires that the monomer concentration exceed a critical value, $a_1 > k'_{d2}/k_+$, set by the balance of elongation and end deactivation. Under the conditions described here, the average

length of the fastest growing distribution is well approximated as $\left[2\left(k_+a_1 - k'_{d2}\right)/k'_{d3}\right]^{1/2}$ as detailed in section 5.4 of the SI.

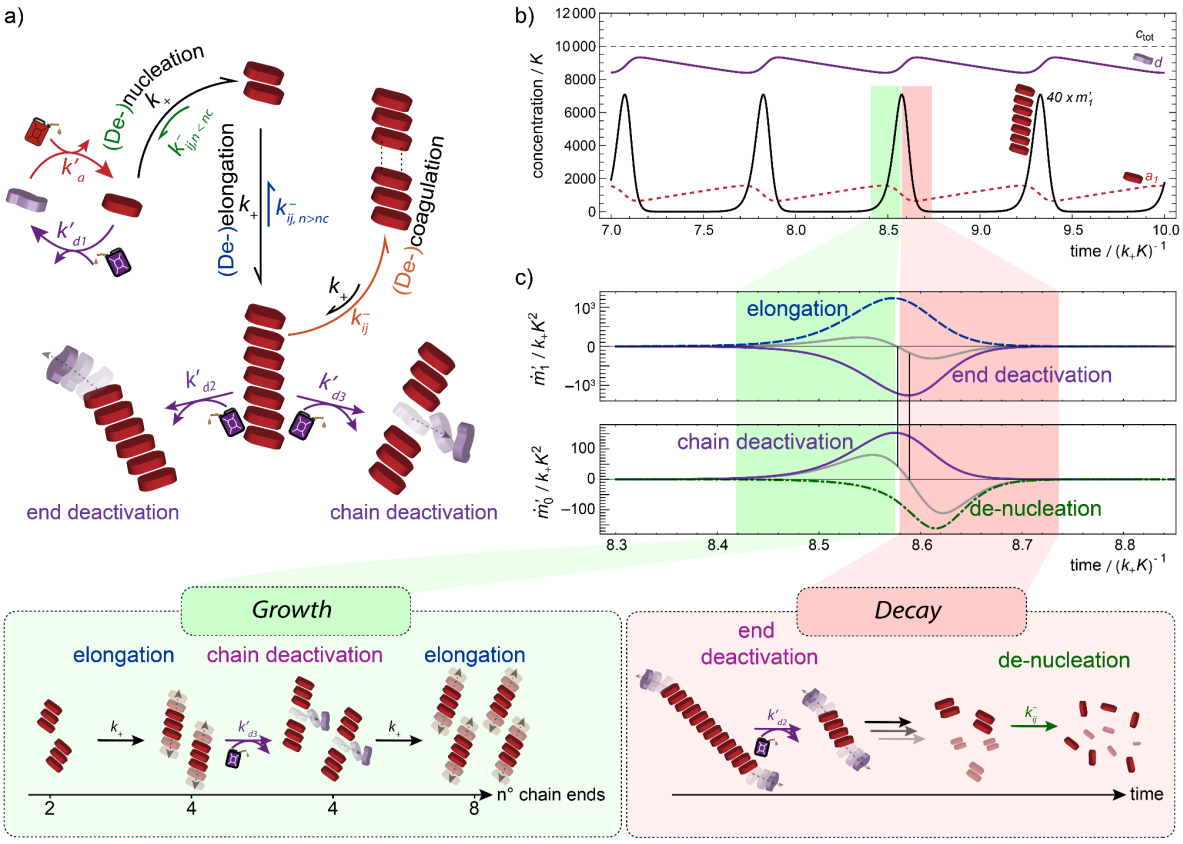

Figure 10 | Chemically-fueled cooperative supramolecular polymerization leading to sustained oscillations. a) Scheme showing the processes involved and their rate constants. De-coagulation is equivalent to thermal fragmentation. b) Dimensionless concentrations of activated monomer a_1, deactivated monomer d, and active monomers embedded inside supramolecular polymers m'_1 (multiplied by 40 for visibility). All show sustained oscillations. c) The rate of production of active monomers inside supramolecular polymers $\dot{m}'_1 = dm'_1/dt$ (top). Positive rates mean activated monomers are polymerizing, whereas negative rates indicate shrinking polymers. The rate of production of the number of polymers $\dot{m}'_0 = dm'_0/dt$ (bottom). Gray lines show the total rates. The insets below show the dominant processes schematically in the growth and decay phase of one oscillation.

5. Conclusions and insights

In recent years, chemically fueled approaches have opened many new perspectives for supramolecular polymers, expanding the scope of the 'traditional' isodesmic and

(anti-)cooperative behavior. Using such approaches—often inspired by natural examples such as microtubules—a new time-dimension has been introduced giving rise to 'Transient Self-assembly'. Supramolecular materials can now appear and disappear autonomously and with high time-precision, which is a unique and new feature as compared to stimuli-responsive (supramolecular) materials.

In this review, we have classified the available literature examples of chemically fueled (one-dimensional) supramolecular polymers undergoing transient self-assembly, by considering their rates of chemical (de)activation and (de)polymerization. In some cases, the examples were 'uncoupled' where only the chemical (de)activation needed to be considered, which we refer to as 'transient activation'. Overall, we have defined four distinct regimes for the latter: I) activation is dominant and fuel abundant, II) deactivation is dominant and fuel abundant, III) deactivation is dominant and fuel sparse, and IV) activation is dominant and fuel sparse. It was interesting to see that even if deactivation is faster than activation, an excess of (activating) fuel could still yield appreciable amounts of self-assembled material (in regime II).

In other cases, there was a clear 'coupling' between the self-assembly processes and the chemical reactivity. For example, the self-assembled structures affect the chemical deactivation reaction by shielding monomers inside bundles of polymers. To better understand such 'coupling', it would be helpful to measure the kinetics of chemical activation and deactivation separately from those of assembly and disassembly; this information is rarely available for the literature examples considered here. More generally, the coupling of reactivity and self-assembly can lead to increasingly rich and interesting behaviors in a variety of materials beyond one-dimensional supramolecular polymers. Klajn and co-workers, for example, showed that nanoparticle assembly leads to 'nanoflasks' where selectivity and reactivity are significantly enhanced.[135]

Going one step further, we have modelled the coupling of simple (isodesmic) polymerization to chemical activation/deactivation, which shows that abundant and long-lived self-assembled structures are possible even in the unfavorable regime III. Though we have only explicitly considered the cases where catalytic activity emerges due to self-assembly or where self-assembly shields monomers from deactivation, other processes frequently found in supramolecular polymers could play a role, e.g.: i) enhanced local concentration and multivalency effects, ii) cooperative catalysis[136], or iii) electronic changes (e.g., a difference in pK_a) due to nearest neighbor interactions. In the coming years, we can expect to see a range of interesting strategies for coupling self-assembly to activation and/or deactivation chemistries.

Lastly, we provided a comprehensive model for supramolecular oscillations in chemically fueled supramolecular polymers. Oscillations are a prototypical emergent property often found in nonlinear systems; to our surprise, we discovered they are feasible in chemically fueled supramolecular polymers. We found sustained oscillations under a continuous influx of chemical fuels, where the following ingredients were found to be vital: i) the polymerization mechanism needs to be highly cooperative, ii) one should work at relatively high concentrations, iii) deactivation along the chain should be much slower than that at the polymer ends (e.g., shielded due to fiber bundling). We believe many systems, even those that have already shown transient self-assembly, could be suitable candidates to obtain supramolecular oscillations. Interestingly, the polymer length distribution periodically violates expectations based on equilibrium self-assembly. In a way, *dissipation* releases the bounds imposed by equilibrium thermodynamics to enable the realization of new materials and dynamic functions.[137]

In contrast to equilibrium materials, for which all processes (e.g., assembly, reaction) are coupled to a common 'thermal bath', future materials that are continuously fueled derive new functionality by coupling their processes to different 'baths'. For example, the 'thermal bath'

governing the mechanical properties of supramolecular structures becomes separate and distinct from the 'chemical bath' governing the rates of polymer assembly and disassembly via chemically fueled processes. Though glimpses of enhanced self-regeneration have been seen in transient self-assembled materials,[138] it is exciting to think about the implications for materials that are continuously fueled. To achieve these materials, better methods are needed to reduce, remove or recycle waste perhaps aided by flow through an artificial vasculature to overcome the limitations of passive diffusive transport[92]. Unlike in natural systems, activating and deactivating fuels often react with one another instead of with the monomer leading to excessive waste production. In addition, (irreversible) side reactions can slowly reduce the available concentration of monomer (or fuel), which limits the number of activation–deactivation cycles that can be achieved. One solution to lower unwanted side reactions (from the chemical fuel) is to use 'pre-fuels' that are only activated catalytically or on-demand (by light for example). In addition, such pre-fuels could help to maintain steady-state conditions for long enough to distinguish which material properties are due to the traditional behavior of the supramolecular polymer and which are due to its chemically fueled behavior.

Another issue is that the study of chemically fueled systems is still done using the same methods and techniques used in traditional (non-dissipative) supramolecular polymers. The number of experimental parameters in fueled systems has, however, greatly increased. That is, not only the supramolecular polymerization but also chemical reactivity and kinetics, fuel concentrations and influx, reactor size and shape, changing medium conditions, and transport phenomena come into play. Automation of experiments using pipetting robots or programmable fluidic circuits is increasingly available and affordable thanks to open-source controller hardware / software (e.g., Arduino, Raspberry Pi, BeagleBone, etc.). For example, syringe pumps[139,140] or pressure-driven pumps[141] are now available at a fraction of the cost due to widely available 3D-

printing and sharing of protocols. Moving from dozens to thousands of experiments is now feasible and much needed to map the large phase space associated with chemically fueled non-equilibrium systems. The analysis of all the data afforded by automation is also becoming more accessible thanks to open-source machine learning (ML) packages (e.g., Scikit, RDKit,…) available on public repositories. Recent examples on prebiotic reaction cycles and (supramolecular) materials show the strength of high-throughput experimentation combined with ML.[142–145] Introducing such tools in the field of chemically fueled systems would make it easier to find emergent behaviors such as oscillations. In addition to automation and ML, Systems Chemistry will continue to rely on chemical kinetic models to provide mechanistic insights into targeted behaviors, guide the design of experimental systems, and direct the deployment of autonomous experiments. Using optimized integration algorithms, such models—for example, those of chemically fueled supramolecular polymerization described here—allow for rapid exploration of system conditions on scales vastly exceeding even high throughput experiments (e.g., 5 million conditions were simulated in 1 hour on a simple desktop computer, see section 5 of the SI). Ultimately, our progress in understanding and designing complex chemical systems will require close integration of all these components: experiment, modeling, data analysis, machine learning, and automation.

By coupling self-assembly to chemical reactions, supramolecular Systems Chemists have unlocked the next level in complexity towards dissipative polymer materials that rival those in nature. We anticipate that further understanding and control over chemically fueled supramolecular polymers will be a key enabler in developing the next generation of interactive (bio)materials.

Acknowledgements:

KJMB and DL were supported as part of the Center for Bio-Inspired Energy Science, an Energy Frontier Research Center funded by the U.S. Department of Energy, Office of Science, Basic

Energy Sciences under Award DE-SC0000989. AS was funded by 'CREANET', a project from the European Union's Horizon 2020 research and innovation programme under the Marie Skłodowska-Curie grant agreement no. 812868. SDP and TMH acknowledge funding from ERC-Starting Grant 'Life-Cycle' project no. 757910. We thank S. Amano for proofreading.

Supporting information:

The Supporting Information is available free of charge online.

Detailed polymerization models without and with chemical fuels

Analysis of literature examples used in the main text

Mathematica scripts for analytical models

The source code for numerical models and a Docker Container with graphical user interface is available at https://github.com/bishopgroup/ChemRevOscillator

References:

(1) Hess, H.; Ross, J. L. Non-Equilibrium Assembly of Microtubules: From Molecules to Autonomous Chemical Robots. *Chem. Soc. Rev.* **2017**, *46*, 5570–5587. https://doi.org/10.1039/C7CS00030H.

(2) Brouhard, G. J.; Rice, L. M. Microtubule Dynamics: An Interplay of Biochemistry and Mechanics. *Nat Rev Mol Cell Biol* **2018**, *19*, 451–463. https://doi.org/10.1038/s41580-018-0009-y.

(3) Holy, T. E.; Dogterom, M.; Yurke, B.; Leibler, S. Assembly and Positioning of Microtubule Asters in Microfabricated Chambers. *PNAS* **1997**, *94*, 6228–6231.

(4) Dogterom, M.; Yurke, B. Microtubule Dynamics and the Positioning of Microtubule Organizing Centers. *Phys. Rev. Lett.* **1998**, *81*, 485–488. https://doi.org/10.1103/PhysRevLett.81.485.

(5) Laan, L.; Pavin, N.; Husson, J.; Romet-Lemonne, G.; van Duijn, M.; López, M. P.; Vale, R. D.; Jülicher, F.; Reck-Peterson, S. L.; Dogterom, M. Cortical Dynein Controls Microtubule Dynamics to Generate Pulling Forces That Position Microtubule Asters. *Cell* **2012**, *148*, 502–514. https://doi.org/10.1016/j.cell.2012.01.007.

(6) Boekhoven, J.; Brizard, A. M.; Kowlgi, K. N. K.; Koper, G. J. M.; Eelkema, R.; van Esch, J. H. Dissipative Self-Assembly of a Molecular Gelator by Using a Chemical Fuel. *Angewandte Chemie International Edition* **2010**, *49*, 4825–4828. https://doi.org/10.1002/anie.201001511.

(7) De, S.; Klajn, R. Dissipative Self-Assembly Driven by the Consumption of Chemical Fuels. *Adv. Mater.* **2018**, *30*, 1706750. https://doi.org/10.1002/adma.201706750.

(8) Weißenfels, M.; Gemen, J.; Klajn, R. Dissipative Self-Assembly: Fueling with Chemicals versus Light. *Chem* **2021**, *7*, 23–37. https://doi.org/10.1016/j.chempr.2020.11.025.
(9) Kariyawasam, L. S.; Hossain, M. M.; Hartley, C. S. The Transient Covalent Bond in Abiotic Nonequilibrium Systems. *Angew. Chem. Int. Ed.* **2021**, *60*, 12648–12658. https://doi.org/10.1002/anie.202014678.
(10) Das, K.; Gabrielli, L.; Prins, L. J. Chemically Fueled Self-Assembly in Biology and Chemistry. *Angew. Chem.* **2021**, *133*, 20280–20303. https://doi.org/10.1002/ange.202100274.
(11) Afrose, S. P.; Ghosh, C.; Das, D. Substrate Induced Generation of Transient Self-Assembled Catalytic Systems. *Chem. Sci.* **2021**. https://doi.org/10.1039/D1SC03492H.
(12) Klajn, R.; Wesson, P. J.; Bishop, K. J. M.; Grzybowski, B. A. Writing Self-Erasing Images Using Metastable Nanoparticle "Inks." *Angewandte Chemie International Edition* **2009**, *48*, 7035–7039. https://doi.org/10.1002/anie.200901119.
(13) Dhiman, S.; Jalani, K.; George, S. J. Redox-Mediated, Transient Supramolecular Charge-Transfer Gel and Ink. *ACS Appl. Mater. Interfaces* **2020**, *12*, 5259–5264. https://doi.org/10.1021/acsami.9b17481.
(14) Tena-Solsona, M.; Rieß, B.; Grötsch, R. K.; Löhrer, F. C.; Wanzke, C.; Käsdorf, B.; Bausch, A. R.; Müller-Buschbaum, P.; Lieleg, O.; Boekhoven, J. Non-Equilibrium Dissipative Supramolecular Materials with a Tunable Lifetime. *Nat Commun* **2017**, *8*, 15895. https://doi.org/10.1038/ncomms15895.
(15) Bai, S.; Niu, X.; Wang, H.; Wei, L.; Liu, L.; Liu, X.; Eelkema, R.; Guo, X.; van Esch, J. H.; Wang, Y. Chemical Reaction Powered Transient Polymer Hydrogels for Controlled Formation and Free Release of Pharmaceutical Crystals. *Chemical Engineering Journal* **2021**, *414*, 128877. https://doi.org/10.1016/j.cej.2021.128877.
(16) Lewis, R. W.; Klemm, B.; Macchione, M.; Eelkema, R. Signal Responsive Transient Coacervation in Complex Coacervate Core Micelles. *ChemRxiv* **2021**. https://doi.org/10.33774/chemrxiv-2021-l3jm1.
(17) Del Grosso, E.; Amodio, A.; Ragazzon, G.; Prins, L. J.; Ricci, F. Dissipative Synthetic DNA-Based Receptors for the Transient Loading and Release of Molecular Cargo. *Angewandte Chemie* **2018**, *130*, 10649–10653. https://doi.org/10.1002/ange.201801318.
(18) Del Grosso, E.; Ragazzon, G.; Prins, L. J.; Ricci, F. Fuel-Responsive Allosteric DNA-Based Aptamers for the Transient Release of ATP and Cocaine. *Angewandte Chemie* **2019**, *131*, 5638–5642. https://doi.org/10.1002/ange.201812885.
(19) Heuser, T.; Weyandt, E.; Walther, A. Biocatalytic Feedback-Driven Temporal Programming of Self-Regulating Peptide Hydrogels. *Angew. Chem. Int. Ed.* **2015**, *54*, 13258–13262. https://doi.org/10.1002/anie.201505013.
(20) Fan, B.; Zhang, K.; Liu, Q.; Eelkema, R. Self-Healing Injectable Polymer Hydrogel via Dynamic Thiol-Alkynone Double Addition Cross-Links. *ACS Macro Lett.* **2020**, *9*, 776–780. https://doi.org/10.1021/acsmacrolett.0c00241.
(21) Solís Muñana, P.; Ragazzon, G.; Dupont, J.; Ren, C. Z.-J.; Prins, L. J.; Chen, J. L.-Y. Substrate-Induced Self-Assembly of Cooperative Catalysts. *Angewandte Chemie International Edition* **2018**, *57*, 16469–16474. https://doi.org/10.1002/anie.201810891.
(22) Chen, R.; Neri, S.; Prins, L. J. Enhanced Catalytic Activity under Non-Equilibrium Conditions. *Nat. Nanotechnol.* **2020**, *15*, 868–874. https://doi.org/10.1038/s41565-020-0734-1.
(23) Amano, S.; Esposito, M.; Kreidt, E.; Leigh, D. A.; Penocchio, E.; Roberts, B. M. W. Insights from an Information Thermodynamics Analysis of a Synthetic Molecular Motor. *Nature Chemistry* **2022**, *14*, 530–537. https://doi.org/10.1038/s41557-022-00899-z.
(24) Penocchio, E.; Rao, R.; Esposito, M. Thermodynamic Efficiency in Dissipative Chemistry. *Nat Commun* **2019**, *10*, 3865. https://doi.org/10.1038/s41467-019-11676-x.
(25) Ragazzon, G.; Prins, L. J. Energy Consumption in Chemical Fuel-Driven Self-Assembly. *Nature Nanotech* **2018**, *13*, 882–889. https://doi.org/10.1038/s41565-018-0250-8.
(26) Arango-Restrepo, A.; Rubi, J. M.; Barragán, D. Understanding Gelation as a Nonequilibrium Self-Assembly Process. *J. Phys. Chem. B* **2018**, *122*, 4937–4945. https://doi.org/10.1021/acs.jpcb.8b02320.
(27) Astumian, R. D. Design Principles for Brownian Molecular Machines: How to Swim in Molasses and Walk in a Hurricane. *Phys. Chem. Chem. Phys.* **2007**, *9*, 5067–5083. https://doi.org/10.1039/B708995C.
(28) Kottas, G. S.; Clarke, L. I.; Horinek, D.; Michl, J. Artificial Molecular Rotors. *Chem. Rev.* **2005**, *105*, 1281–1376. https://doi.org/10.1021/cr0300993.

(29) Shandilya, E.; Maiti, S. Deconvolution of Transient Species in a Multivalent Fuel-Driven Multistep Assembly under Dissipative Conditions. *ChemSystemsChem* **2020**, *2*. https://doi.org/10.1002/syst.201900040.
(30) van der Helm, M. P.; de Beun, T.; Eelkema, R. On the Use of Catalysis to Bias Reaction Pathways in Out-of-Equilibrium Systems. *Chem. Sci.* **2021**, *12*, 4484–4493. https://doi.org/10.1039/D0SC06406H.
(31) Rieß, B.; Grötsch, R. K.; Boekhoven, J. The Design of Dissipative Molecular Assemblies Driven by Chemical Reaction Cycles. *Chem* **2020**, *6*, 552–578. https://doi.org/10.1016/j.chempr.2019.11.008.
(32) Wang, G.; Liu, S. Strategies to Construct a Chemical-Fuel-Driven Self-Assembly. *ChemSystemsChem* **2020**, *2*, e1900046. https://doi.org/10.1002/syst.201900046.
(33) Heuser, T.; Steppert, A.-K.; Molano Lopez, C.; Zhu, B.; Walther, A. Generic Concept to Program the Time Domain of Self-Assemblies with a Self-Regulation Mechanism. *Nano Lett.* **2015**, *15*, 2213–2219. https://doi.org/10.1021/nl5039506.
(34) Fialkowski, M.; Bishop, K. J. M.; Klajn, R.; Smoukov, S. K.; Campbell, C. J.; Grzybowski, B. A. Principles and Implementations of Dissipative (Dynamic) Self-Assembly. *J. Phys. Chem. B* **2006**, *110*, 2482–2496. https://doi.org/10.1021/jp054153q.
(35) Insua, I.; Montenegro, J. Synthetic Supramolecular Systems in Life-like Materials and Protocell Models. *Chem* **2020**, *6*, 1652–1682. https://doi.org/10.1016/j.chempr.2020.06.005.
(36) Mattia, E.; Otto, S. Supramolecular Systems Chemistry. *Nature Nanotech* **2015**, *10*, 111–119. https://doi.org/10.1038/nnano.2014.337.
(37) Maity, I.; Wagner, N.; Mukherjee, R.; Dev, D.; Peacock-Lopez, E.; Cohen-Luria, R.; Ashkenasy, G. A Chemically Fueled Non-Enzymatic Bistable Network. *Nat Commun* **2019**, *10*, 4636. https://doi.org/10.1038/s41467-019-12645-0.
(38) Morrow, S. M.; Colomer, I.; Fletcher, S. P. A Chemically Fuelled Self-Replicator. *Nat Commun* **2019**, *10*, 1011. https://doi.org/10.1038/s41467-019-08885-9.
(39) Colomer, I.; Morrow, S. M.; Fletcher, S. P. A Transient Self-Assembling Self-Replicator. *Nat Commun* **2018**, *9*, 2239. https://doi.org/10.1038/s41467-018-04670-2.
(40) Wang, C.; Chen, Q.; Wang, Z.; Zhang, X. An Enzyme-Responsive Polymeric Superamphiphile. *Angewandte Chemie* **2010**, *122*, 8794–8797. https://doi.org/10.1002/ange.201004253.
(41) Heinen, L.; Heuser, T.; Steinschulte, A.; Walther, A. Antagonistic Enzymes in a Biocatalytic PH Feedback System Program Autonomous DNA Hydrogel Life Cycles. *Nano Lett.* **2017**, *17*, 4989–4995. https://doi.org/10.1021/acs.nanolett.7b02165.
(42) Dong, B.; Liu, L.; Hu, C. ATP-Driven Temporal Control over Structure Switching of Polymeric Micelles. *Biomacromolecules* **2018**, *19*, 3659–3668. https://doi.org/10.1021/acs.biomac.8b00769.
(43) Green, L. N.; Subramanian, H. K. K.; Mardanlou, V.; Kim, J.; Hariadi, R. F.; Franco, E. Autonomous Dynamic Control of DNA Nanostructure Self-Assembly. *Nat. Chem.* **2019**, *11*, 510–520. https://doi.org/10.1038/s41557-019-0251-8.
(44) Muradyan, H.; Guan, Z. Chemothermally Driven Out-of-Equilibrium Materials for Macroscopic Motion. *ChemSystemsChem* **2020**, *2*, e2000024. https://doi.org/10.1002/syst.202000024.
(45) van Haren, M.; Nakashima, K.; Spruijt, E. Coacervate-Based Protocells: Integration of Life-Like Properties in a Droplet. *Journal of Systems Chemistry* **2020**, *8*, 107–120.
(46) Geng, W.-C.; Liu, Y.-C.; Zheng, Z.; Ding, D.; Guo, D.-S. Direct Visualization and Real-Time Monitoring of Dissipative Self-Assembly by Synchronously Coupled Aggregation-Induced Emission. *Mater. Chem. Front.* **2017**, *1*, 2651–2655. https://doi.org/10.1039/C7QM00407A.
(47) te Brinke, E.; Groen, J.; Herrmann, A.; Heus, H. A.; Rivas, G.; Spruijt, E.; Huck, W. T. S. Dissipative Adaptation in Driven Self-Assembly Leading to Self-Dividing Fibrils. *Nature Nanotech* **2018**, *13*, 849–855. https://doi.org/10.1038/s41565-018-0192-1.
(48) Dambenieks, A. K.; Vu, P. H. Q.; Fyles, T. M. Dissipative Assembly of a Membrane Transport System. *Chem. Sci.* **2014**, *5*, 3396–3403. https://doi.org/10.1039/C4SC01258E.
(49) Kariyawasam, L. S.; Hartley, C. S. Dissipative Assembly of Aqueous Carboxylic Acid Anhydrides Fueled by Carbodiimides. *J. Am. Chem. Soc.* **2017**, *139*, 11949–11955. https://doi.org/10.1021/jacs.7b06099.
(50) Hossain, M. M.; Atkinson, J. L.; Hartley, C. S. Dissipative Assembly of Macrocycles Comprising Multiple Transient Bonds. *Angew. Chem. Int. Ed.* **2020**, *59*, 13807–13813. https://doi.org/10.1002/anie.202001523.

(51) Go, D.; Rommel, D.; Liao, Y.; Haraszti, T.; Sprakel, J.; Kuehne, A. J. C. Dissipative Disassembly of Colloidal Microgel Crystals Driven by a Coupled Cyclic Reaction Network. *Soft Matter* **2018**, *14*, 910–915. https://doi.org/10.1039/C7SM02061A.
(52) Cheng, G.; Perez-Mercader, J. Dissipative Self-Assembly of Dynamic Multicompartmentalized Microsystems with Light-Responsive Behaviors. *Chem* **2020**, *6*, 1160–1171. https://doi.org/10.1016/j.chempr.2020.02.009.
(53) Maiti, S.; Fortunati, I.; Ferrante, C.; Scrimin, P.; Prins, L. J. Dissipative Self-Assembly of Vesicular Nanoreactors. *Nature Chem* **2016**, *8*, 725–731. https://doi.org/10.1038/nchem.2511.
(54) Post, E. A. J.; Fletcher, S. P. Dissipative Self-Assembly, Competition and Inhibition in a Self-Reproducing Protocell Model. *Chem. Sci.* **2020**, *11*, 9434–9442. https://doi.org/10.1039/D0SC02768E.
(55) van Ravensteijn, B. G. P.; Hendriksen, W. E.; Eelkema, R.; van Esch, J. H.; Kegel, W. K. Fuel-Mediated Transient Clustering of Colloidal Building Blocks. *J. Am. Chem. Soc.* **2017**, *139*, 9763–9766. https://doi.org/10.1021/jacs.7b03263.
(56) della Sala, F.; Maiti, S.; Bonanni, A.; Scrimin, P.; Prins, L. J. Fuel-Selective Transient Activation of Nanosystems for Signal Generation. *Angew. Chem. Int. Ed.* **2018**, *57*, 1611–1615. https://doi.org/10.1002/anie.201711964.
(57) Choi, S.; Mukhopadhyay, R. D.; Kim, Y.; Hwang, I.; Hwang, W.; Ghosh, S. K.; Baek, K.; Kim, K. Fuel-Driven Transient Crystallization of a Cucurbit[8]Uril-Based Host–Guest Complex. *Angew. Chem.* **2019**, *131*, 17006–17009. https://doi.org/10.1002/ange.201910161.
(58) Lagzi, I.; Kowalczyk, B.; Wang, D.; Grzybowski, B. A. Nanoparticle Oscillations and Fronts. *Angewandte Chemie International Edition* **2010**, *49*, 8616–8619. https://doi.org/10.1002/anie.201004231.
(59) von Maltzahn, G.; Min, D.-H.; Zhang, Y.; Park, J.-H.; Harris, T. J.; Sailor, M.; Bhatia, S. N. Nanoparticle Self-Assembly Directed by Antagonistic Kinase and Phosphatase Activities. *Adv. Mater.* **2007**, *19*, 3579–3583. https://doi.org/10.1002/adma.200701183.
(60) Helm, M. P.; Wang, C.; Fan, B.; Macchione, M.; Mendes, E.; Eelkema, R. Organocatalytic Control over a Fuel-Driven Transient-Esterification Network**. *Angew. Chem.* **2020**, *132*, 20785–20792. https://doi.org/10.1002/ange.202008921.
(61) Osypova, A.; Dübner, M.; Panzarasa, G. Oscillating Reactions Meet Polymers at Interfaces. *Materials* **2020**, *13*, 2957. https://doi.org/10.3390/ma13132957.
(62) Sawczyk, M.; Klajn, R. Out-of-Equilibrium Aggregates and Coatings during Seeded Growth of Metallic Nanoparticles. *J. Am. Chem. Soc.* **2017**, *139*, 17973–17978. https://doi.org/10.1021/jacs.7b09111.
(63) van Ravensteijn, B. G. P.; Voets, I. K.; Kegel, W. K.; Eelkema, R. Out-of-Equilibrium Colloidal Assembly Driven by Chemical Reaction Networks. *Langmuir* **2020**, *36*, 10639–10656. https://doi.org/10.1021/acs.langmuir.0c01763.
(64) Hao, X.; Chen, L.; Sang, W.; Yan, Q. Periodically Self-Pulsating Microcapsule as Programmed Microseparator via ATP-Regulated Energy Dissipation. *Adv. Sci.* **2018**, *5*, 1700591. https://doi.org/10.1002/advs.201700591.
(65) Rakotondradany, F.; Whitehead, M. A.; Lebuis, A.-M.; Sleiman, H. F. Photoresponsive Supramolecular Systems: Self-Assembly of Azodibenzoic Acid Linear Tapes and Cyclic Tetramers. *Chem. Eur. J.* **2003**, *9*, 4771–4780. https://doi.org/10.1002/chem.200304864.
(66) Vialetto, J.; Anyfantakis, M.; Rudiuk, S.; Morel, M.; Baigl, D. Photoswitchable Dissipative Two-Dimensional Colloidal Crystals. *Angew. Chem. Int. Ed.* **2019**, *58*, 9145–9149. https://doi.org/10.1002/anie.201904093.
(67) Roy, S.; Roy, S.; Rao, A.; Devatha, G.; Pillai, P. P. Precise Nanoparticle–Reactant Interaction Outplays Ligand Poisoning in Visible-Light Photocatalysis. *Chem. Mater.* **2018**, *30*, 8415–8419. https://doi.org/10.1021/acs.chemmater.8b03108.
(68) Warren, S. C.; Guney-Altay, O.; Grzybowski, B. A. Responsive and Nonequilibrium Nanomaterials. *J. Phys. Chem. Lett.* **2012**, *3*, 2103–2111. https://doi.org/10.1021/jz300584c.
(69) Nakashima, K. K.; Baaij, J. F.; Spruijt, E. Reversible Generation of Coacervate Droplets in an Enzymatic Network. *Soft Matter* **2018**, *14*, 361–367. https://doi.org/10.1039/C7SM01897E.
(70) Arango-Restrepo, A.; Barragán, D.; Rubi, J. M. Self-Assembling Outside Equilibrium: Emergence of Structures Mediated by Dissipation. *Phys. Chem. Chem. Phys.* **2019**, *21*, 17475–17493. https://doi.org/10.1039/C9CP01088B.

(71) Yoshida, R.; Takahashi, T.; Yamaguchi, T.; Ichijo, H. Self-Oscillating Gel. *J. Am. Chem. Soc.* **1996**, *118*, 5134–5135. https://doi.org/10.1021/ja9602511.
(72) Ueki, T.; Shibayama, M.; Yoshida, R. Self-Oscillating Micelles. *Chem. Commun.* **2013**, *49*, 6947. https://doi.org/10.1039/c3cc38432b.
(73) Tamate, R.; Ueki, T.; Shibayama, M.; Yoshida, R. Self-Oscillating Vesicles: Spontaneous Cyclic Structural Changes of Synthetic Diblock Copolymers. *Angew. Chem. Int. Ed.* **2014**, *53*, 11248–11252. https://doi.org/10.1002/anie.201406953.
(74) Wang, G.; Liu, S. Strategies to Construct a Chemical-Fuel-Driven Self-Assembly. *ChemSystemsChem* **2020**, *2*. https://doi.org/10.1002/syst.201900046.
(75) Wang, H.; Wang, Y.; Shen, B.; Liu, X.; Lee, M. Substrate-Driven Transient Self-Assembly and Spontaneous Disassembly Directed by Chemical Reaction with Product Release. *J. Am. Chem. Soc.* **2019**, *141*, 4182–4185. https://doi.org/10.1021/jacs.8b12777.
(76) Wang, G.; Tang, B.; Liu, Y.; Gao, Q.; Wang, Z.; Zhang, X. The Fabrication of a Supra-Amphiphile for Dissipative Self-Assembly. *Chem. Sci.* **2016**, *7*, 1151–1155. https://doi.org/10.1039/C5SC03907J.
(77) Ouyang, Y.; Zhang, P.; Manis-Levy, H.; Paltiel, Y.; Willner, I. Transient Dissipative Optical Properties of Aggregated Au Nanoparticles, CdSe/ZnS Quantum Dots, and Supramolecular Nucleic Acid-Stabilized Ag Nanoclusters. *J. Am. Chem. Soc.* **2021**, *143*, 17622–17632. https://doi.org/10.1021/jacs.1c07895.
(78) Lagzi, I.; Wang, D.; Kowalczyk, B.; Grzybowski, B. A. Vesicle-to-Micelle Oscillations and Spatial Patterns. *Langmuir* **2010**, *26*, 13770–13772. https://doi.org/10.1021/la102635w.
(79) Urban, M. W. *Handbook of Stimuli-Responsive Materials*; John Wiley & Sons, 2011.
(80) Adams, D. J.; Butler, M. F.; Frith, W. J.; Kirkland, M.; Mullen, L.; Sanderson, P. A New Method for Maintaining Homogeneity during Liquid–Hydrogel Transitions Using Low Molecular Weight Hydrogelators. *Soft Matter* **2009**, *5*, 1856–1862. https://doi.org/10.1039/B901556F.
(81) Bal, S.; Das, K.; Ahmed, S.; Das, D. Chemically Fueled Dissipative Self-Assembly That Exploits Cooperative Catalysis. *Angew. Chem. Int. Ed.* **2019**, *58*, 244–247. https://doi.org/10.1002/anie.201811749.
(82) Ashkenasy, G.; Hermans, T. M.; Otto, S.; Taylor, A. F. Systems Chemistry. *Chem. Soc. Rev.* **2017**, *46*, 2543–2554. https://doi.org/10.1039/C7CS00117G.
(83) Amano, S.; Borsley, S.; Leigh, D. A.; Sun, Z. Chemical Engines: Driving Systems Away from Equilibrium through Catalyst Reaction Cycles. *Nat. Nanotechnol.* **2021**, *16*, 1057–1067. https://doi.org/10.1038/s41565-021-00975-4.
(84) Magnasco, M. O. Molecular Combustion Motors. *Phys. Rev. Lett.* **1994**, *72*, 2656–2659. https://doi.org/10.1103/PhysRevLett.72.2656.
(85) Astumian, R. D.; Bier, M. Mechanochemical Coupling of the Motion of Molecular Motors to ATP Hydrolysis. *Biophysical Journal* **1996**, *70*, 637–653. https://doi.org/10.1016/S0006-3495(96)79605-4.
(86) Raeburn, J.; Zamith Cardoso, A.; Adams, D. J. The Importance of the Self-Assembly Process to Control Mechanical Properties of Low Molecular Weight Hydrogels. *Chem. Soc. Rev.* **2013**, *42*, 5143. https://doi.org/10.1039/c3cs60030k.
(87) Panja, S.; Patterson, C.; Adams, D. J. Temporally-Programmed Transient Supramolecular Gels. *Macromol. Rapid Commun.* **2019**, 1900251. https://doi.org/10.1002/marc.201900251.
(88) Panja, S.; Fuentes-Caparrós, A. M.; Cross, E. R.; Cavalcanti, L.; Adams, D. J. Annealing Supramolecular Gels by a Reaction Relay. *Chem. Mater.* **2020**, *32*, 5264–5271. https://doi.org/10.1021/acs.chemmater.0c01483.
(89) Panzarasa, G.; Torzynski, A. L.; Sai, T.; Smith-Mannschott, K.; Dufresne, E. R. Transient Supramolecular Assembly of a Functional Perylene Diimide Controlled by a Programmable PH Cycle. *Soft Matter* **2020**, *16*, 591–594. https://doi.org/10.1039/C9SM02026H.
(90) Panzarasa, G.; Sai, T.; Torzynski, A. L.; Smith-Mannschott, K.; Dufresne, E. R. Supramolecular Assembly by Time-Programmed Acid Autocatalysis. *Mol. Syst. Des. Eng.* **2020**, *5*, 445–448. https://doi.org/10.1039/C9ME00139E.
(91) Jain, A.; Dhiman, S.; Dhayani, A.; Vemula, P. K.; George, S. J. Chemical Fuel-Driven Living and Transient Supramolecular Polymerization. *Nat Commun* **2019**, *10*, 450. https://doi.org/10.1038/s41467-019-08308-9.
(92) Sorrenti, A.; Leira-Iglesias, J.; Sato, A.; Hermans, T. M. Non-Equilibrium Steady States in Supramolecular Polymerization. *Nat Commun* **2017**, *8*, 15899. https://doi.org/10.1038/ncomms15899.

(93) Spitzer, D.; Rodrigues, L. L.; Straßburger, D.; Mezger, M.; Besenius, P. Tuneable Transient Thermogels Mediated by a PH- and Redox-Regulated Supramolecular Polymerization. *Angew. Chem. Int. Ed.* **2017**, *56*, 15461–15465. https://doi.org/10.1002/anie.201708857.
(94) Olivieri, E.; Quintard, G.; Naubron, J.-V.; Quintard, A. Chemically Fueled Three-State Chiroptical Switching Supramolecular Gel with Temporal Control. *J. Am. Chem. Soc.* **2021**, *143*, 12650–12657. https://doi.org/10.1021/jacs.1c05183.
(95) Mishra, A.; Korlepara, D. B.; Kumar, M.; Jain, A.; Jonnalagadda, N.; Bejagam, K. K.; Balasubramanian, S.; George, S. J. Biomimetic Temporal Self-Assembly via Fuel-Driven Controlled Supramolecular Polymerization. *Nat Commun* **2018**, *9*, 1295. https://doi.org/10.1038/s41467-018-03542-z.
(96) Dhiman, S.; Jain, A.; Kumar, M.; George, S. J. Adenosine-Phosphate-Fueled, Temporally Programmed Supramolecular Polymers with Multiple Transient States. *J. Am. Chem. Soc.* **2017**, *139*, 16568–16575. https://doi.org/10.1021/jacs.7b07469.
(97) Mondal, S.; Podder, D.; Nandi, S. K.; Chowdhury, S. R.; Haldar, D. Acid-Responsive Fibrillation and Urease-Assisted Defibrillation of Phenylalanine: A Transient Supramolecular Hydrogel. *Soft Matter* **2020**, *16*, 10115–10121. https://doi.org/10.1039/D0SM00774A.
(98) Angulo-Pachón, C. A.; Miravet, J. F. Sucrose-Fueled, Energy Dissipative, Transient Formation of Molecular Hydrogels Mediated by Yeast Activity. *Chem. Commun.* **2016**, *52*, 5398–5401. https://doi.org/10.1039/C6CC01183G.
(99) Mukhopadhyay, R. D.; Choi, S.; Sen, S. K.; Hwang, I.; Kim, K. Transient Self-assembly Processes Operated by Gaseous Fuels under Out-of-Equilibrium Conditions. *Chem. Asian J.* **2020**, *15*, 4118–4123. https://doi.org/10.1002/asia.202001183.
(100) Afrose, S. P.; Bal, S.; Chatterjee, A.; Das, K.; Das, D. Designed Negative Feedback from Transiently Formed Catalytic Nanostructures. *Angew. Chem. Int. Ed.* **2019**, *58*, 15783–15787. https://doi.org/10.1002/anie.201910280.
(101) Pappas, C. G.; Sasselli, I. R.; Ulijn, R. V. Biocatalytic Pathway Selection in Transient Tripeptide Nanostructures. *Angew. Chem. Int. Ed.* **2015**, *54*, 8119–8123. https://doi.org/10.1002/anie.201500867.
(102) Debnath, S.; Roy, S.; Ulijn, R. V. Peptide Nanofibers with Dynamic Instability through Nonequilibrium Biocatalytic Assembly. *J. Am. Chem. Soc.* **2013**, *135*, 16789–16792. https://doi.org/10.1021/ja4086353.
(103) Kumar, M.; Ing, N. L.; Narang, V.; Wijerathne, N. K.; Hochbaum, A. I.; Ulijn, R. V. Amino-Acid-Encoded Biocatalytic Self-Assembly Enables the Formation of Transient Conducting Nanostructures. *Nature Chem* **2018**, *10*, 696–703. https://doi.org/10.1038/s41557-018-0047-2.
(104) Singh, N.; Lainer, B.; Formon, G. J. M.; De Piccoli, S.; Hermans, T. M. Re-Programming Hydrogel Properties Using a Fuel-Driven Reaction Cycle. *J. Am. Chem. Soc.* **2020**, *142*, 4083–4087. https://doi.org/10.1021/jacs.9b11503.
(105) Singh, N.; Lopéz-Acosta, Á.; Formon, G.; Hermans, T. Chemically Fueled Self-Sorted Hydrogels. *J. Am. Chem. Soc.* **2022**, *144*, 410–415. https://doi.org/10.1021/jacs.1c10282.
(106) Tena-Solsona, M.; Wanzke, C.; Riess, B.; Bausch, A. R.; Boekhoven, J. Self-Selection of Dissipative Assemblies Driven by Primitive Chemical Reaction Networks. *Nat Commun* **2018**, *9*, 2044. https://doi.org/10.1038/s41467-018-04488-y.
(107) Rieß, B.; Wanzke, C.; Tena-Solsona, M.; Grötsch, R. K.; Maity, C.; Boekhoven, J. Dissipative Assemblies That Inhibit Their Deactivation. *Soft Matter* **2018**, *14*, 4852–4859. https://doi.org/10.1039/C8SM00822A.
(108) Grötsch, R. K.; Angı, A.; Mideksa, Y. G.; Wanzke, C.; Tena-Solsona, M.; Feige, M. J.; Rieger, B.; Boekhoven, J. Dissipative Self-Assembly of Photoluminescent Silicon Nanocrystals. *Angew. Chem. Int. Ed.* **2018**, *57*, 14608–14612. https://doi.org/10.1002/anie.201807937.
(109) Wanzke, C.; Jussupow, A.; Kohler, F.; Dietz, H.; Kaila, V. R. I.; Boekhoven, J. Dynamic Vesicles Formed By Dissipative Self-Assembly. *ChemSystemsChem* **2020**, *2*. https://doi.org/10.1002/syst.201900044.
(110) Kriebisch, C. M. E.; Bergmann, A. M.; Boekhoven, J. Fuel-Driven Dynamic Combinatorial Libraries. *J. Am. Chem. Soc.* **2021**, *143*, 7719–7725. https://doi.org/10.1021/jacs.1c01616.
(111) Grötsch, R. K.; Wanzke, C.; Speckbacher, M.; Angı, A.; Rieger, B.; Boekhoven, J. Pathway Dependence in the Fuel-Driven Dissipative Self-Assembly of Nanoparticles. *J. Am. Chem. Soc.* **2019**, *141*, 9872–9878. https://doi.org/10.1021/jacs.9b02004.

(112) Kriebisch, B. A. K.; Jussupow, A.; Bergmann, A. M.; Kohler, F.; Dietz, H.; Kaila, V. R. I.; Boekhoven, J. Reciprocal Coupling in Chemically Fueled Assembly: A Reaction Cycle Regulates Self-Assembly and Vice Versa. *J. Am. Chem. Soc.* **2020**, *142*, 20837–20844. https://doi.org/10.1021/jacs.0c10486.
(113) Dai, K.; Fores, J. R.; Wanzke, C.; Winkeljann, B.; Bergmann, A. M.; Lieleg, O.; Boekhoven, J. Regulating Chemically Fueled Peptide Assemblies by Molecular Design. *J. Am. Chem. Soc.* **2020**, *142*, 14142–14149. https://doi.org/10.1021/jacs.0c04203.
(114) Dai, K.; Fores, J. R.; Wanzke, C.; Winkeljann, B.; Bergmann, A. M.; Lieleg, O.; Boekhoven, J. Regulating Chemically Fueled Peptide Assemblies by Molecular Design. *J. Am. Chem. Soc.* **2020**, *142*, 14142–14149. https://doi.org/10.1021/jacs.0c04203.
(115) Wojciechowski, J. P.; Martin, A. D.; Thordarson, P. Kinetically Controlled Lifetimes in Redox-Responsive Transient Supramolecular Hydrogels. *J. Am. Chem. Soc.* **2018**, *140*, 2869–2874. https://doi.org/10.1021/jacs.7b12198.
(116) Ogden, W. A.; Guan, Z. Redox Chemical-Fueled Dissipative Self-Assembly of Active Materials. *ChemSystemsChem* **2020**, *2*, e1900030. https://doi.org/10.1002/syst.201900030.
(117) Boekhoven, J.; Hendriksen, W. E.; Koper, G. J. M.; Eelkema, R.; Esch, J. H. van. Transient Assembly of Active Materials Fueled by a Chemical Reaction. *Science* **2015**, *349*, 1075–1079. https://doi.org/10.1126/science.aac6103.
(118) Footer, M. J.; Kerssemakers, J. W. J.; Theriot, J. A.; Dogterom, M. Direct Measurement of Force Generation by Actin Filament Polymerization Using an Optical Trap. *Proceedings of the National Academy of Sciences* **2007**, *104*, 2181–2186. https://doi.org/10.1073/pnas.0607052104.
(119) Kerssemakers, J. W. J.; Laura Munteanu, E.; Laan, L.; Noetzel, T. L.; Janson, M. E.; Dogterom, M. Assembly Dynamics of Microtubules at Molecular Resolution. *Nature* **2006**, *442*, 709–712. https://doi.org/10.1038/nature04928.
(120) Dogterom, M.; Kerssemakers, J. W.; Romet-Lemonne, G.; Janson, M. E. Force Generation by Dynamic Microtubules. *Current Opinion in Cell Biology* **2005**, *17*, 67–74. https://doi.org/10.1016/j.ceb.2004.12.011.
(121) Krawczyk, J.; Kierfeld, J. Stall Force of Polymerizing Microtubules and Filament Bundles. *EPL* **2011**, *93*, 28006. https://doi.org/10.1209/0295-5075/93/28006.
(122) Kubota, R.; Makuta, M.; Suzuki, R.; Ichikawa, M.; Tanaka, M.; Hamachi, I. Force Generation by a Propagating Wave of Supramolecular Nanofibers. *Nat Commun* **2020**, *11*, 3541. https://doi.org/10.1038/s41467-020-17394-z.
(123) Mandelkow, E.-M.; Mandelkow, E. Microtubule Oscillations. *Cell Motility* **1992**, *22*, 235–244. https://doi.org/10.1002/cm.970220403.
(124) Lange, G.; Mandelkow, E.-M.; Jagla, A.; Mandelkow, E. Tubulin Oligomers and Microtubule Oscillations. *European Journal of Biochemistry* **1988**, *178*, 61–69. https://doi.org/10.1111/j.1432-1033.1988.tb14429.x.
(125) Cantekin, S. Consequences of Cooperativity in Supramolecular Polymers. Phd Thesis (Research TU/e / Graduation TU/e), Technische Universiteit Eindhoven, Eindhoven, 2012. https://doi.org/10.6100/IR732936.
(126) Mes, T.; Cantekin, S.; Balkenende, D. W. R.; Frissen, M. M. M.; Gillissen, M. A. J.; De Waal, B. F. M.; Voets, I. K.; Meijer, E. W.; Palmans, A. R. A. Thioamides: Versatile Bonds To Induce Directional and Cooperative Hydrogen Bonding in Supramolecular Polymers. *Chemistry – A European Journal* **2013**, *19*, 8642–8649. https://doi.org/10.1002/chem.201204273.
(127) Kulkarni, C.; Meijer, E. W.; Palmans, A. R. A. Cooperativity Scale: A Structure–Mechanism Correlation in the Self-Assembly of Benzene-1,3,5-Tricarboxamides. *Acc. Chem. Res.* **2017**, *50*, 1928–1936. https://doi.org/10.1021/acs.accounts.7b00176.
(128) Perrin, D. D. The Effect of Temperature on PK Values of Organic Bases. *Aust. J. Chem.* **1964**, *17*, 484–488. https://doi.org/10.1071/ch9640484.
(129) Epstein, I. R.; Pojman, J. A. *An Introduction to Nonlinear Chemical Dynamics: Oscillations, Waves, Patterns, and Chaos*; Oxford University Press, 1998.
(130) Cross, M.; Greenside, H. *Pattern Formation and Dynamics in Nonequilibrium Systems*; Cambridge University Press, 2009.
(131) Heinen, L.; Walther, A. Programmable Dynamic Steady States in ATP-Driven Nonequilibrium DNA Systems. *Science Advances 5*, eaaw0590. https://doi.org/10.1126/sciadv.aaw0590.

(132) Leira-Iglesias, J.; Tassoni, A.; Adachi, T.; Stich, M.; Hermans, T. M. Oscillations, Travelling Fronts and Patterns in a Supramolecular System. *Nature Nanotech* **2018**, *13*, 1021–1027. https://doi.org/10.1038/s41565-018-0270-4.
(133) Carnall, J. M. A.; Waudby, C. A.; Belenguer, A. M.; Stuart, M. C. A.; Peyralans, J. J.-P.; Otto, S. Mechanosensitive Self-Replication Driven by Self-Organization. *Science* **2010**, *327*, 1502–1506. https://doi.org/10.1126/science.1182767.
(134) Colomb-Delsuc, M.; Mattia, E.; Sadownik, J. W.; Otto, S. Exponential Self-Replication Enabled through a Fibre Elongation/Breakage Mechanism. *Nat Commun* **2015**, *6*, 7427. https://doi.org/10.1038/ncomms8427.
(135) Zhao, H.; Sen, S.; Udayabhaskararao, T.; Sawczyk, M.; Kučanda, K.; Manna, D.; Kundu, P. K.; Lee, J.-W.; Král, P.; Klajn, R. Reversible Trapping and Reaction Acceleration within Dynamically Self-Assembling Nanoflasks. *Nature Nanotech* **2016**, *11*, 82–88. https://doi.org/10.1038/nnano.2015.256.
(136) Peters, R. *Cooperative Catalysis: Designing Efficient Catalysts for Synthesis*; John Wiley & Sons, 2015.
(137) Dou, Y.; Dhatt-Gauthier, K.; Bishop, K. J. M. Thermodynamic Costs of Dynamic Function in Active Soft Matter. *Current Opinion in Solid State and Materials Science* **2019**, *23*, 28–40. https://doi.org/10.1016/j.cossms.2018.11.002.
(138) Boekhoven, J.; Hendriksen, W. E.; Koper, G. J. M.; Eelkema, R.; van Esch, J. H. Transient Assembly of Active Materials Fueled by a Chemical Reaction. *Science* **2015**, *349*, 1075–1079. https://doi.org/10.1126/science.aac6103.
(139) Baas, S.; Saggiomo, V. Ender3 3D Printer Kit Transformed into Open, Programmable Syringe Pump Set. *HardwareX* **2021**, *10*, e00219. https://doi.org/10.1016/j.ohx.2021.e00219.
(140) Lake, J. R.; Heyde, K. C.; Ruder, W. C. Low-Cost Feedback-Controlled Syringe Pressure Pumps for Microfluidics Applications. *PLOS ONE* **2017**, *12*, e0175089. https://doi.org/10.1371/journal.pone.0175089.
(141) Lupinski, T.; Ludwig, M.; Fraden, S.; Tompkins, N. An Arduino-Based Constant Pressure Fluid Pump. *Eur. Phys. J. E* **2021**, *44*, 14. https://doi.org/10.1140/epje/s10189-020-00002-9.
(142) Banerjee, R.; Phan, A.; Wang, B.; Knobler, C.; Furukawa, H.; O'Keeffe, M.; Yaghi, O. M. High-Throughput Synthesis of Zeolitic Imidazolate Frameworks and Application to CO2 Capture. *Science* **2008**, *319*, 939–943. https://doi.org/10.1126/science.1152516.
(143) Potyrailo, R.; Rajan, K.; Stoewe, K.; Takeuchi, I.; Chisholm, B.; Lam, H. Combinatorial and High-Throughput Screening of Materials Libraries: Review of State of the Art. *ACS Comb. Sci.* **2011**, *13*, 579–633. https://doi.org/10.1021/co200007w.
(144) Kelty, M. L.; Morris, W.; Gallagher, A. T.; Anderson, J. S.; Brown, K. A.; Mirkin, C. A.; Harris, T. D. High-Throughput Synthesis and Characterization of Nanocrystalline Porphyrinic Zirconium Metal–Organic Frameworks. *Chem. Commun.* **2016**, *52*, 7854–7857. https://doi.org/10.1039/C6CC03264H.
(145) Greenaway, R. L.; Santolini, V.; Bennison, M. J.; Alston, B. M.; Pugh, C. J.; Little, M. A.; Miklitz, M.; Eden-Rump, E. G. B.; Clowes, R.; Shakil, A.; Cuthbertson, H. J.; Armstrong, H.; Briggs, M. E.; Jelfs, K. E.; Cooper, A. I. High-Throughput Discovery of Organic Cages and Catenanes Using Computational Screening Fused with Robotic Synthesis. *Nat Commun* **2018**, *9*, 2849. https://doi.org/10.1038/s41467-018-05271-9.